MNRAS **000**, 1–?? (2015) Preprint 11 May 2016 Compiled using MNRAS LATEX style file v3.0

Application of USNO-B1.0 towards selecting objects with displaced blue and red components

Joel S. Jayson[1]⋆
[1]*P.O. Box 34, Brooklyn, N.Y 11235, USA*

arXiv:1605.03037v1 [astro-ph.IM] 10 May 2016

11 May 2016

ABSTRACT

We have conducted a feasibility study to determine the effectiveness of using USNO-B1.0 data to preferentially detect objects with displaced red and blue components. A procedure was developed to search catalogue entries for such objects, which include M dwarfs paired with white dwarfs or with earlier main-sequence stars, and galaxies with asymmetric colour distributions. Residual differences between red and blue and infrared and blue scanned emulsion images define vectors, which, when appropriately aligned and of sufficient length, signal potential candidates. Test sample sets were analysed to evaluate the effective discrimination of the technique. Over 91,000 USNO-B1.0 catalogue entries at points throughout the celestial sphere were then filtered for acceptable combinations of entry observations and magnitudes and the resulting total of about 17,000 entries was winnowed down to a little more than 200 objects of interest. These were screened by visual examination of photo images to a final total of 146 candidates. About one quarter of these candidates coincide with SDSS data. Those constituents fall into two groups, single and paired objects. SDSS identified several galaxies in the first group. Regarding the second group, at least half of its members were tentatively identified as main-sequence pairs, the greater portion being of widely separated spectral types. Two white dwarf–main-sequence pairs were also identified. Most importantly, the vectors formed from USNO-B1.0 residuals were in alignment with corresponding SDSS pair position angles, thereby supporting this work's central thesis.

Key words: methods: data analysis – binaries: visual – WDs–galaxies: starburst

1 INTRODUCTION

With USNO-B1.0 the United States Naval Observatory (USNO) presented a catalogue of over 7400 scanned Schmidt plates exposed in surveys that spanned a period from 1949 to 2002 (Monet et al. 2003). The catalogue represents a culmination of the photographic era of observation. We develop a means of selecting objects with displaced red and blue components through analysis of USNO-B1.0 entry fields. (The catalogue is hereafter referred to in the text as USNO-B). Christy, Wellnitz & Currie (1983) first proposed a method of detecting binaries with different coloured components by employing a shift in position dependent upon the observation band. Others (Sorokin & Tokovinin 1985; Wielen 1996; Bailey 1998) further investigated the phenomenon and Pourbaix et al. (2004) were first to successfully detect a number of binary systems on the basis of such colour differentiation, deriving their candidates from Sloan Digital Sky Survey (SDSS) Data Release 2 entries.

Entities anticipated to be singled out include M dwarfs (dM) paired with early main-sequence stars, white dwarfs (WDs) paired with main-sequence stars and galaxies with asymmetric colour distribution such as those with extensive stellar nurseries. The preferential selection of main-sequence pairs with widely spaced spectral types lends itself to studies of low mass ratio binaries (Fischer & Marcy 1992; Clarke 2009; Forgan & Rice 2011; Reggiani & Meyer 2013; Duchêne & Kraus 2013). By-products of the procedure include distant blue objects, red giant/carbon stars or galaxies in angular proximity to main-sequence stars. In concept the technique, augmented with x-ray survey data, could further detect young neutron star–main-sequence binaries. However, the paucity of such objects makes this latter possibility unlikely.

Central to the technique, the pair of stars or galaxy must appear as a single object in all observations of the USNO-B entry. (Though the proximity of two stellar objects is more likely to indicate a binary association than a chance occurrence, other than when discussing known binaries, we generally use the term 'pair''or pairing' to describe

⋆ E-mail: jsjayson@yahoo.com

© 2015 The Authors

two objects in angular proximity). Our initial focus is on three test groups. We then follow-up by extracting paired and galactic candidates from USNO-B entries taken at spot locations throughout the celestial sphere.

The USNO-B catalogue has over one billion object entries in two epochs, with two colour magnitude readings for the first epoch and three colour readings for the second epoch. The deep photographic surveys captured objects as faint as magnitude 21. The resulting image sizes range from about 2.5 arcsec across for a magnitude V=20 object to approximately 12 arcsec for magnitude 13 (King & Raff 1977). Because bright objects were saturated, entities brighter than V=13 were replaced in the USNO-B catalogue by Tycho-2 readings (Høg et al. 2000), where available. Those replacement entries are not of interest here.

To determine which observations belonged to an entry, USNO first passed a search aperture of 3 arcsec through the assembled digital files. Two or more points located within the aperture were entered as a record. Identification of objects with large proper motions (pms) required opening the search aperture and entailed a more involved procedure. Entries vary from a minimum of two observations to a maximum of five. See Monet et al. (2003) for further details. Residual values in the mean observation epoch are listed for each observation, i.e., the arcsec deviation of both RA (α) and Dec (δ) from their mean values (the RA deviation,$15\Delta\alpha\cos\delta$, is the negative x residual). We identify the sought after paired and galactic candidates through analysis of the residuals. The catalogue, when supplemented with the survey logs[1], furnishes enough data, including computed pm, to enable retrieval of the observation coordinates. The dispersion at the mean observation epoch is about 0.12 arcsec. For a discussion of absolute errors see Roeser, Demleitner & Schilbach (2010).

We would not expect the residuals to vary much from 0.12 arcsec for a single star. Also, because of the rigid relationship between main-sequence stellar mass, radius and radiative intensity, when a main-sequence pairing appears on the emulsion as a single compact object we expect the centre of the object image to follow the more massive star regardless of exposure colour. Again, the residuals are anticipated to be of the order of the measurement errors. However, a significant proviso to this conclusion obtains when the pair is measured as a single object, but appears on the emulsion as an extended object, i.e., two abutting or overlapping entities. In that circumstance, if the two stars are of widely separated spectral types the red–blue displacement will be detected.

For a WD–main-sequence pairing the rigid main-sequence relationship no longer applies. A hot WD emits at a greater intensity, yet because of its small radius, it is not necessarily more luminous. The blue exposure is displaced from the red exposure and that shift will lead to larger residual values. A similar argument applies for a galaxy with a displacement of large active and quiescent regions.

That is the effect, in brief, that is central to our procedure. In fact, there are other factors that can lead to large residuals. The USNO in their effort to capture many objects erred on the side of gathering together data points that did not belong to the same entity. Often the giveaway for such a hybrid will be large residuals. None the less, a distinction can usually be made between legitimate objects and these hybrids by several means, e.g., comparing magnitudes at a given colour from one epoch to the other, seeking anomalies in data plotted in the observation epochs, and by use of images and finder charts from the USNO website.

SDSS has charted about 35 per cent of the sky in five colours and with unprecedented photometric precision (York et al. 2000; Abazajian et al. 2003; Ahn et al. 2012). Its primary purpose was collecting massive data on quasars and galaxies. Adjuncts to the programme have generated extensive WD catalogues (Kleinman et al. 2013). In addition to the colour induced displacement work of Pourbaix et al. (2004), Smolčić et al. (2004) identified compact WD–main-sequence binaries by analysis of colour magnitudes across several bands . Over 2,500 such systems have been catalogued (Rebassa-Mansergas et al. 2012, 2013; Li et al. 2014).

USNO-B represents an older technology. Its photometry is over an order of magnitude coarser than that of SDSS. However, USNO-B is a comprehensive catalogue that encompasses the entire celestial sphere, which is a major reason for pursuing this feasibility study.

Section 2 establishes criteria to detect candidate entries. In Section 3 groups of known single stars, dM binaries and WD–dM binaries are probed to test our approach and outlier points are analysed. The entries studied in Section 3 each have five observations. Section 4 considers candidate identification from USNO-B listings with four observations and for one combination of three observations. The insights gained in Sections 3 and 4 are put to use in Section 5 where USNO-B entries from various sectors of the sky are sifted for objects of interest. Section 6 analyses the segment of the candidate population coincident with SDSS data. That data provides star/galaxy identification and, through use of colour–colour plots, affords tentative typing of candidate pairings. We present our conclusions in Section 7.

2 CRITERIA FOR DETECTION OF OBJECTS OF INTEREST

2.1 The USNO-B data set and a measure of a blue-red shift

Table 1 summarizes the various surveys that contributed to USNO-B and is adapted from the USNO-B catalogue. A USNO-B entry contains 51 fields. Assuming that there is a full complement of five observations, about half of those fields are of immediate interest. Table 2 provides abbreviated entries for the two objects depicted in Fig. 1. An alternate object designation (not provided in the USNO-B catalogue), and the object coordinates constitute the first three rows, followed by the mean observation epoch and the USNO computed pm components. All succeeding rows refer to individual observations. They include the survey number, the survey field, the date of the observation (not provided in the USNO-B catalogue, obtained from the survey log), the x residual and the y residual.

[1] Most survey logs are available at the USNO web site, `www.usno.navy.mil/USNO/astrometry/optical-IR-prod/icas`. A complete set of survey logs was furnished courtesy of David G. Monet, USNO, Flagstaff Station

Table 1. Surveys used for USNO-B1.0. SERC-I* supplements POSS-IIN and is an extension of the SERC-I survey (Monet et al. 2003).

No.	Name	Λ (nm)	Obs. dates
0	POSS-IO	350-500	1949-1965
1	POSS-IE	620-670	1949-1965
2	POSS-IIJ	385-540	1985-2000
3	POSS-IIF	610-690	1985-1999
4	SERC-J	385-540	1978-1990
5	ESO-R	630-690	1974-1994
6	AAO-R	590-690	1985-1998
7	POSS-IIN	730-900	1989-2000
8	SERC-I	715-900	1978-2002
9	SERC-I*	715-900	1981-2002

Table 2. Data for two objects plotted in Fig. 1. USNO-B1.0 0611-0011923 is a single star. USNO-B1.0 1187-0163669 is a WD–dM binary whose components are WD 0824+288 and PG 0824+289B. Coordinates are at equinox J2000, epoch J2000.

	USNO-B1.0 identities	
	0611-0011923	1187-0163669
Alt. Designation	GJ 1031	WD 0824+288 & dM
RA (^{h} ^{m} ^{s}.)	01 08 18.28	08 27 05.14
Dec ($^\circ$ $'$ $''$.)	-28 48 20.09	28 44 02.65
Mean epoch of obs.	1972.9	1977.9
RA pm	724 mas yr^{-1}	0 mas yr^{-1}
Dec pm	-110 mas yr^{-1}	0 mas yr^{-1}
B1 survey	0	0
B1 field	884	312
B1 obs. date	1955.9	1955.2
B1 x residual	0.03 arcsec	0.02 arcsec
B1 y residual	-0.14 arcsec	0.40 arcsec
R1 survey	1	1
R1 field	884	312
R1 obs. date	1955.9	1955.2
R1 x residual	-0.01 arcsec	-0.42 arcsec
R1 y residual	0.07 arcsec	0.11 arcsec
B2 survey	4	2
B2 field	412	431
B2 obs. date	1977.6	1990.2
B2 x residual	-0.13 arcsec	0.62 arcsec
B2 y residual	0.02 arcsec	0.17 arcsec
R2 survey	6	3
R2 field	412	431
R2 obs. date	1994,6	1989.7
R2 x residual	0.03 arcsec	-0.01 arcsec
R2 y residual	-0.12 arcsec	-0.25 arcsec
I2 survey	8	7
I2 field	412	431
I2 obs. date	1980.7	1999.2
I2 x residual	0.05 arcsec	-0.24 arcsec
I2 y residual	0.16 arcsec	-0.46 arcsec

A most useful measure gauges the relative displacement between the blue images and the corresponding red images and also, with regard to second epoch exposures, the relative displacement between the second epoch blue and infrared images. Concerning that relative displacement, consider surveys 0 and 1. Those are the blue and red surveys, respectively, of the first Palomar Observatory Sky Survey (POSS-I, see Minkowski & Abell (1963)) . What is unique about these readings is that the blue and red plates for each field were exposed on the same night. Thus, beyond the measurement error, the difference between the red and blue x and y readings gives a direct indication of the displacement between the two images in the observation epoch, as well as any other epoch that they both may be transformed to. For all other surveys, the difference in exposure dates between different colour plates within the same epoch vary from as little as a negligible amount to as much as 20 yr. Since the residuals are given in the mean epoch of the object observations, in theory the difference in exposure dates is transformed away. However, that transformation depends upon the USNO-B computed pm. Any error in computed pm will translate to a corresponding error in location, the error being equal to the product of the pm error times the difference in observation dates. Large pm's play a role in the vicinity of the solar neighbourhood. However, a good fraction of the USNO-B entries constitute distant objects with zero or close to zero pm.

In Fig. 1 the residuals are plotted for two very different objects. In Fig. 1a they are plotted for GJ 1031, a single star. Here *R1* and *B1* refer, respectively, to the epoch 1 red and blue exposure residual values and *R2*, *B2* and *I2* are the corresponding epoch 2 red, blue and infrared residual values. Displacement vectors are drawn for ***R1-B1***, ***R2-B2*** and ***I2-B2***, with the tail of the vector at the blue position. The data points are clustered within a small area and the vectors are directed in random directions.

In Fig. 1b the residuals are plotted for a WD–dM binary. The WD component is WD 0824+288 and the dM component PG 0824+289B. In this instance the three vectors are aligned in nearly the same direction and the magnitudes of the vectors are significantly larger than those of Fig. 1a.

Table 2 lists a USNO-B pm value of zero for the WD 0824+288, PG 0824+289B system. A glance at Fig. 1b indicates that the pm value is in fact not zero. We surmise that the USNO-B algorithm may have set the pm to zero because of a contradiction in the RA terms.

To demonstrate the relative position of the displacement vectors with respect to the two stars, we compute an approximate corrected pm and transform all observations to ICRS, epoch 2003.07 to put them in the same reference frame and epoch as that of the stellar positions taken from SDSS data release nine. For comparison with the SDSS data the USNO-B coordinates require corrections to the ICRS frame (Roeser et al. 2010), which can be found at the German Astrophysical Virtual Observatory (GAVO)[2]. Since the USNO-B pm is zero, the residuals represent the relative positions in the observation epochs as well as in the mean epoch. We compute an approximate pm by taking the differences of the second epoch blue and red observations with their corresponding observations in the first epoch, *B2-B1* and *R2-R1*, dividing by the differences in observation dates and taking a weighed average. Using the computed value of 16 mas yr^{-1} at a position angle of 240°, the residuals are transformed and plotted in Fig. 1c. The displacement vectors align in good agreement with the WD–dM position angle. The slight offset between the displacement vectors and the binary reflects

[2] http://dc.zah.uni-heidelberg.de/ppmxl/q/corr/info

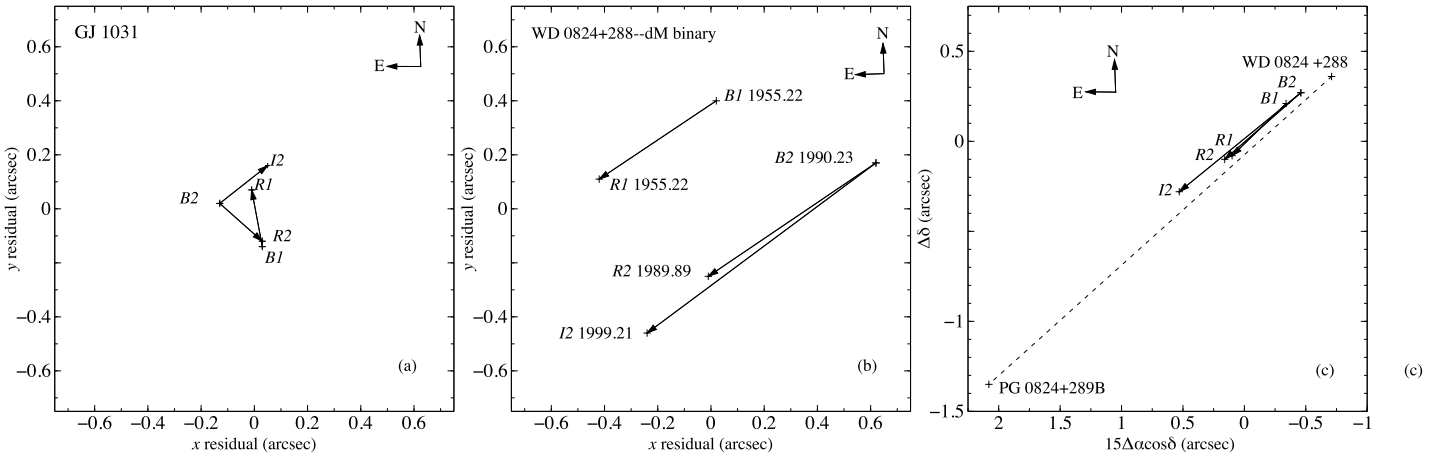

Figure 1. Residuals for a single star and for a WD–dM binary. The residuals are plotted in the mean epoch of observation in panes (a) and (b), 1972.9 and 1977.9, respectively. They are plotted on the same scale for ready comparison. The observation dates for the WD–dM binary are noted in pane (b). These are put to use for the transformation indicated in pane (c). The origin in pane (c) is at the USNO-B1.0 1187-0163669 ICRS, epoch 2003.07 position, $08^h27^m05^s.10+ 28^\circ44'02''.4$ as determined using GAVO corrections and a computed pm. See text for further discussion.

the approximate nature of the pm computation and the bias of the displacement vectors towards the WD signifies that that star is much brighter than its dM companion.

The WD 0824+288, PG 0824+289B system provides an introduction into what can be extracted from USNO-B. We next develop the specific criteria for gleaning candidate objects from the general population of USNO-B entries.

2.2 A Point Count Approach for Evaluating Potential Candidates

Though the displacement vectors in Figs. 1b and 1c present a clear picture of the binary system, they embody a 'noise' component as well as a 'signal', Fig. 1a providing some idea of that noise level. To get a more quantitative reading, the mean and sample deviation of the rms residual radius are computed for a sample of 40 single stars where,

$$r_{rms} = sqrt((x_1^2 + y_1^2 + x_2^2 + y_2^2 + ...x_5^2 + y_5^2)/5). \quad (1)$$

In this equation x_1, x_2...and y_1, y_2... represent the negative RA residual component ($15\Delta\alpha\cos\delta$) and the Dec residual component, respectively, of the observations that constitute an entry. The sample stars all have five observations

The USNO-B identity, a standard identity, coordinates and the computed rms residual radius for each of these stars is provided in Table A1. The last column of this table, listing point counts, is addressed in Section 3. To ensure that the stars in this group are indeed single, the sample was selected from the solar neighbourhood, no further than 20 pc, a region where extensive exploration extends some confidence. [One object, GJ 4360, is a barely resolved dM binary (Montagnier et al. 2006), which with an angular separation of ∼0.1 arcsec, for all practical purposes stands in as a single star in this exercise.] The selection was dictated in large part by brightness, since many stars at that close range were replaced in the USNO catalogue by Tycho-2 readings. dMs predominate along with a couple of WDs. Since only USNO-B entries with five observations were included that further limited the selection sample. The mean r_{rms} for the sample falls very much as expected, at 0.14 arcsec with a sample deviation of 0.05 arcsec.

Referring to Figs. 1b and 1c, we readily spell out the requirements for an entry with five observations:

(i) The magnitude of each displacement vector should be significantly larger than 0.15 arcsec, yet not so restricted as to to eliminate closely spaced pairs. We choose a minimum of 0.3 arcsec.

(ii) The angle between any two displacement vectors must fall below some maximum cutoff. Here we use a nominal noise level of 0.15 arcsec and for each displacement vector ($\boldsymbol{DV}$) allow an angular deviation of arctan(0.15/|$\boldsymbol{DV}$|). That expression is obtained by assuming a worst case of the noise component in quadrature with the signal component. By adding the maximum allowed deviation from alignment for each of two vectors we arrive at a comfortable margin of error where the allowed angular deviation between two displacement vectors must be less than arctan(0.15/|$\boldsymbol{DV1}$|)+arctan(0.15/|$\boldsymbol{DV2}$|). The larger the vectors, the tighter the angular deviation restriction. Alternatively, a small displacement vector magnitude leads to a loose restriction. We address that problem below.

(iii) As seen in Figs. 1b and 1c, if the object is a legitimate candidate then, |$\boldsymbol{I2\text{-}B2}$|> |$\boldsymbol{R2\text{-}B2}$|.

A point system with these requirements leads to a maximum of three points for satisfying minimum displacement vector magnitudes and a maximum of three points for satisfying the condition on restricted angular deviations. We address condition (iii) as follows: |$\boldsymbol{I2\text{-}B2}$| >|$\boldsymbol{R2\text{-}B2}$| =1 point; 0.2 arcsec>|$\boldsymbol{R2\text{-}B2}$|-|$\boldsymbol{I2\text{-}B2}$|>0=0 points; |$\boldsymbol{R2\text{-}B2}$|-|$\boldsymbol{I2\text{-}B2}$|>0.2 arcsec= -1 point. Regarding small displacement vector magnitudes, if any |$\boldsymbol{DV}$| <0.15 arcsec, then for the two angles that that vector forms with the other two vectors, the angular deviation point count is zero. The displacement vectors are limited to residual differences between

observations in the same epoch. See Section 4.2 for a short discussion of mixed epoch vectors.

Before putting these requirements to trial with a population of unknowns, we evaluate them first on known quantities in the following section.

3 TEST SAMPLES AND ANALYSIS OF OUTLIERS

We anticipate that our point system will select paired main-sequence stars with extended USNO-B images and of widely separated spectral types. WD–dM pairs are expected to be selected, even if their USNO-B images are compact. However, selection of dM binaries is not considered likely regardless of emulsion image extension. Three sample groups, each of 40 objects, are evaluated to test these expectations, single stars, dM binaries and WD–dM binaries. Each object comprises five observations. The single star group is the same as that represented in Table A1 and is included as a benchmark. The binary sample group members are listed in Table A2.

Janson et al. (2012, 2014) have conducted a large-scale study of multiple dM systems using earth bound telescopes, but obtaining diffraction limited resolution through the use of speckle imaging. Table A2 provides the USNO-B identity, a standard identity for one of the components, coordinates, the component separation and the computed point counts for 40 of these systems. Systems were selected with separations greater than a few tenths of an arcsec and less than 7.5 arcsec.

The sample of WD–dM binaries, found in Table A2, derived from several sources. Farihi et al. (2006, 2010) conducted a study with the *Hubble Space Telescope* in which over forty systems were resolved into two or more components. Hoard et al. (2007) established a table of WD–low mass star binaries acquired from a culmination of work entailing analysis of the McCook & Scion (1999) catalogue using 2 Micron All Sky Survey (2MASS) photometry, Skrutskie et al. (2006) and follow up telescopic surveys. Silvestri et al. (2005) compiled a table of WD–dM wide binaries in the course of a study on the age of such systems. In all these instances we selected samples with separation distances from several tenths of an arcsec to 10 arcsec. Table A2 indicates whether or not SDSS data is available for the WD–dM entries.

Fig. 2 provides histograms for the three groups of samples, the single stars in Fig. 2a, the binary M-dwarfs in Fig. 2b and the WD–dM binaries in Fig. 2c. There are no point counts of 6 or 7 for the first two groups, while the third, the group of WD–dM binaries, has a total of 18 objects at those levels and an additional 6 objects with a point count of 5. That is an encouraging result, but it leaves open the question of why the contrast is not even more extreme. The outliers are investigated in the following three subsections. These are the objects in the first two groups with point counts of 4 and 5, and the objects in the third group with point counts 5 and lower.

3.1 Single Star Outliers

In Fig. 2a four stars exhibit a point count of 4 and three a point count of 5. Two of the stars with point count 5 and one of the stars with point count 4 exhibit diffraction spikes on the USNO-B images. Monet et al. (2003), in explaining the reason for substitution of Tycho-2 entries for bright stars, state that the USNO precision measuring machine's measures are 'usually confused by... gross saturation, diffraction spikes and halos.' Eliminating from consideration USNO-B bright stars that weren't captured by Tycho-2 would partially resolve this problem. That option is adopted in Section 5. Diffraction spikes from neighbouring stars remain an issue.

At the other extreme, LP 888-18, a star with point count 5, has a *B1* magnitude of 20.71 and a *B2* magnitude of 19.96. We attribute the large displacement vectors and high point count of this star to the less precise measurements at the higher magnitudes. An upper limit of 19.5 *B2* magnitude will be introduced in section 5. Large spreads in magnitude, such as in the blue in this instance, are not uncommon in USNO-B. Monet et al. (2003) give a standard deviation of 0.25 mag. For eligibility into the sample groups objects were required to differ by less than one magnitude in the red and in the blue.

A large fraction of the stars in Fig. 2a have point counts of 1, 2 or 3. These stars have short displacement vectors, but not necessarily shorter than the angular deviation cutoff of 0.15 arcsec. As a result moderate sized angular deviations are awarded points. Additionally, if the residuals are solely due to measurement errors we can expect that for half of these objects $|\boldsymbol{I2\text{-}B2}|>|\boldsymbol{R2\text{-}B2}|$, and hence another point will be awarded. It is therefore not surprising that a few objects with rms residual radii in the vicinity of 0.12 arcsec none the less register point counts of four. The remaining three objects fall into this category.

However, that is not the full extent of the problem. All three of these stars have an inclusive angle of less than 11° between the ***R2-B2*** and ***I2-B2*** vectors. For that matter, six of the seven outlier stars fall into this category and of the forty stars in the sample, twelve have an inclusive angle of less than 15°. By comparison, for the ***R1-B1*** and ***I2-B2*** vectors, four of the forty stars satisfy that condition and for the ***R1-B1*** and ***R2-B2*** vectors two out of forty do.

R2-B2 and ***I2-B2*** are not totally independent vectors, both sharing the common *B2* point. Given three observation points, and deviations due to measurement errors alone, assume one of the measurements more errant than the other two. When that point is *B2*, we expect that the two vectors formed from *B2* will be closely aligned. This explanation satisfies the statistics, although the sample size is limited. This is a serious problem if the number of false candidates is to be minimized. It is especially so when, as will be discussed in Section 4, searches are to be conducted using only the two epoch 2 vectors. We expect that the longer the displacement vectors, the less likely the effect. Aside from requiring longer displacement vectors, a cap on the *B2* magnitude, discussed above, will further alleviate the problem.

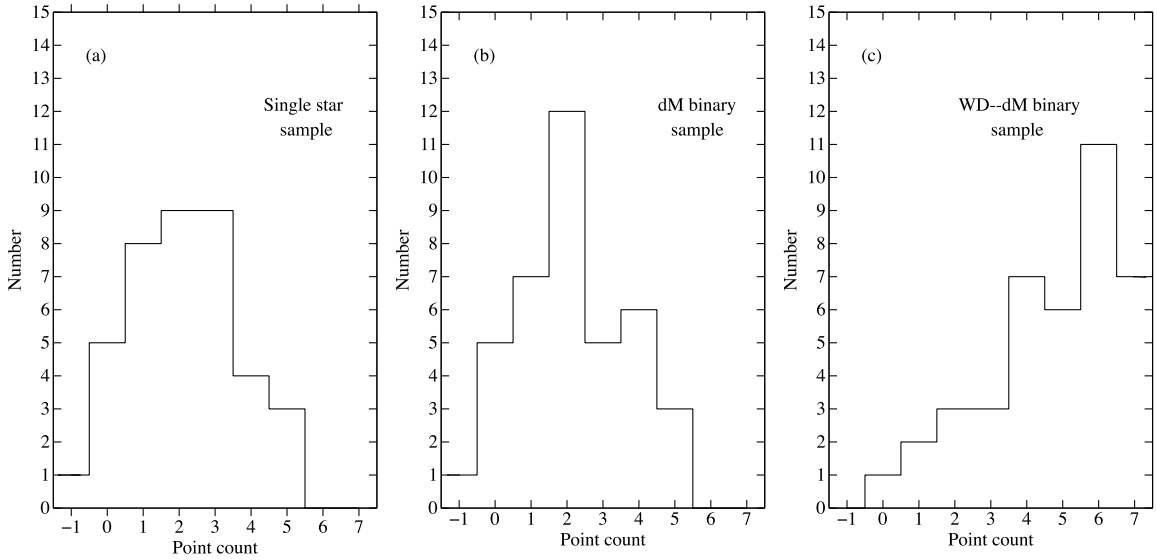

Figure 2. Histograms for single star, dM binary and WD–dM binary sample sets. The WD–dM sample set shows a distinct bias towards higher point counts.

3.2 dM binary outliers

In Fig. 2b six objects have a point count 4 and three a point count 5. Two of the point count 4 objects display prominent diffraction spikes as does one with a point count of 5. Another point count 4 binary falls into the category of an object with small residuals resulting in random angular deviations that are awarded points.

The other five objects of interest have large point counts because the passage of a neighbouring star, not a member of the binary, affects the results. We take a close look at two of these objects.

3.2.1 2MASS J05191382-0059423

Figure 3 depicts downloaded USNO images at the 2MASS J05191382-0059423 position. In the 0 and 1 survey images, shown respectively in Figs. 3a and 3b, the object identified by USNO-B is in fact two objects. The segment to the south-east (north is up, east is to the left) exhibits little change from the blue image to red. The second segment increases its size significantly on the red exposure. It is that object that has the coordinates of 2MASS J05191382-0059423 and within that object lies the binary system, with a separation of 1.1 arcsec, that we originally set out to probe. Further, Fig 3c displays the image from survey 3. The first two surveys were conducted in 1953.91. Survey 3 was conducted in 1991.79 and indicates either the apparent orbiting of the 'blue' and 'red' objects or one object passing the other. They have an angular separation of roughly ∼7 arcsec. According to Janson et al. (2014) the distance of the 'red' object is about 31 pc, which, if the objects are part of the same system, translates to a separation of ∼200 au. The total mass of the two red companions is 0.65 $M_\odot$ (Janson et al. 2012) and if the objects are gravitationally bound the 'blue' object is likely a WD with mass of the order of $M_\odot$ and the system has a period on the order of 3000 yr. In a span of 38 yr the objects have changed their orientation by about 45 degrees. We are probably observing a fly-by. The 'blue' object has SDSS and 2MASS identities, SDSS J051913.68-005949.9 and 2MASS J05191367-0059499.

3.2.2 2MASS J05464932-0757427

USNO-B images at the 2MASS J05464932-0757427 position indicate the blending of two star images with the passage of time. A plot of the data in the observation epochs (Fig. 4) delineates the situation. The epoch 2 red and infrared data points reflect the blended image while all other data points refer to the separate objects. USNO-B has two entries. The one associated with 2MASS J0546932-0757427 is USNO-B1.0 0820-0079747, which has five data points, and is the entry under analysis. The second entry, USNO-B1.0 0820-0079746 is associated with a southern object, 2MASS J05464930-0757494 and has three data points. The blending of the two images, with the concurrent southward shift of the *R2* and *I2* points results in two aligned and large epoch 2 displacement vectors, and a count of 4 points.

3.3 WD–dM binary outliers

For the WD–dM binary sample group the outliers are the entries with the low point counts as contrasted with the other two sample groups. Twenty-two entries out of forty have point counts below 6. The low point count entries fall into a few major groups: large pair angular separation, small pair angular separation, large magnitude spread between the pair components, tight angular constraints between the displacement vectors and miscellaneous. A summary follows, again, a pair is referred to by just one component:

(i) Six entries with pair component angular separations ranging from 5 to 10 arcsec, display as separate entities on all observation images or as a mix, separate on at least one image and blended on at least one image. We require a blended object on all images for the displacement vectors to properly

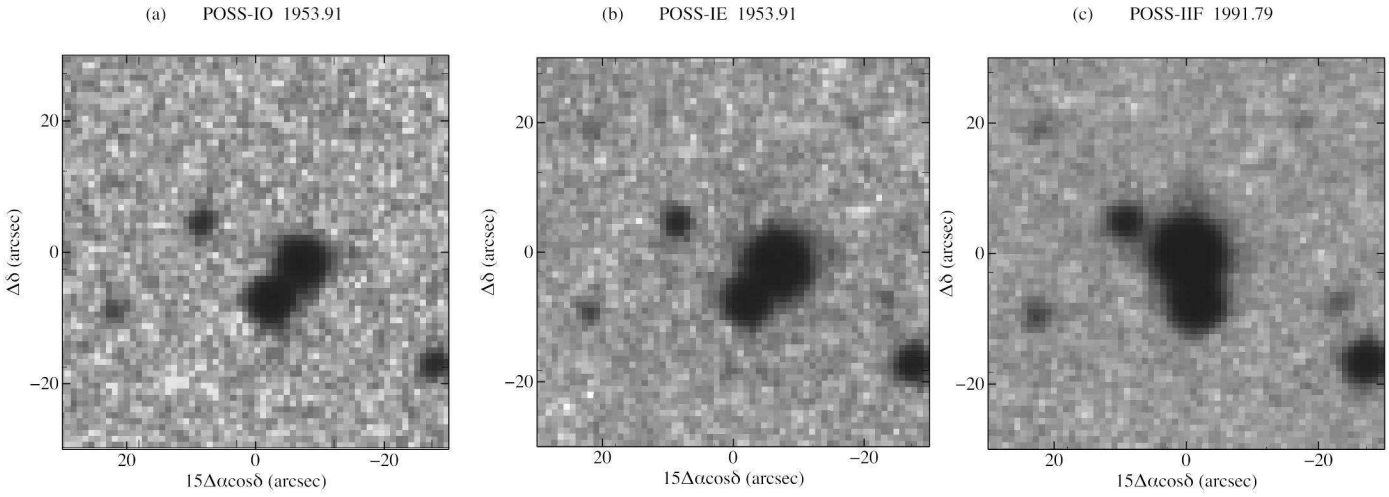

Figure 3. USNO-B1.0 images for 2MASS J05191382-0059423. All images are shown in equinox J2000, epoch J2000. The observation dates are indicated above each pane. The centre coordinate for each is $05^h19^m14^s.35$ -00°59′38″.0. See text for detailed description.

reflect the presence of red and blue components. Three entries in the sample group, WD 0325+263 and WD 1402+506, each with point count 6, and WD 2341-164 with point count 7, have separations of 6-6.3, 5 and 6.2-6.7 arcsec respectively, giving some indication of how large a separation can yield positive results.

(ii) Three entries with pair component separations less than 0.7 arcsec failed to achieve 6 or 7 points. In all three instances the main problem lies with one or more short displacement vectors, which is not unexpected. Two entries in the sample group, WD 1443+337 and WD 1558+616, each with point counts of 6, have respective pair component separations of 0.68 and 0.72 arcsec, providing some measure of the minimal separation that can be detected.

(iii) For eight entries one stellar component dominates throughout the three colour spectrum, leading to a low point count.

(iv) Two entries lost points because their large displacement vectors resulted in tight constraints on angular alignment. Thus, the position angles for the three WD 0949+451 vectors ranged from 102°to 124°, yet two points were deducted on this account.

(v) WD 1240+754 is highlighted here because of an artefact that appears, improbably, on the POSS-IE exposure as an extension to the binary system. WD 1619+525 is a multiple star system. Two of the displacement vectors roughly align with the far companion. ***R1-B1*** is over 120°out of alignment. Hoard et al. (2007) made a tentative identification of WD 2318-137, point count 3, as a binary in their table 2 and this system would not have been considered for inclusion in the sample group except that the tentative assignment stemmed from observation of elongations in the POSS red images. We confirm moderate sized displacement vectors (0.25 to 0.48 arcsec). However, the vector position angles are unaligned.

4 CRITERIA FOR USNO-B ENTRIES WITH THREE OR FOUR OBSERVATIONS

4.1 Two displacement vector criteria

Objects with five observations provide an opportunity for verification through several variables. Since there were no first epoch blue plate exposures taken south of -33° declination we must also address four object detections. That is also true in the north if a greater portion of the catalogue is to be accessed. Three object observations are also considered under one circumstance.

No more than two displacement vectors can be formed from four observations. (An epoch 2 vector could be formed from ***I2-R2***, but that does not appear promising to us and will not be considered). Entries limited to N=3 can be assessed only in the instance when all three observations are from epoch 2, in which situation we can compare ***R2-B2*** with ***I2-B2***. Beyond entries with five observations, the additional possibilities are: (*B1,R1,B2,R2*), (*B1,R1,B2,I2*), (*B1,B2,R2,I2*), (*R1,B2,R2,I2*) and (*B2,R2,I2*).

With less than five observations there is little opportunity for assigning points. Two displacement vectors and their position angle difference yield three points. A fourth point is assigned for $|\boldsymbol{I2\text{-}B2}|>|\boldsymbol{R2\text{-}B2}|$ for those entries with all three epoch 2 observations. That extra point in no way reflects the relative value of the pairing of two epoch 2 vectors versus an ***R1-B1*** vector paired with an epoch 2 vector. The latter is a more reliable indicator as both vectors are completely independent. In all situations with fewer than five observations the minimum displacement vector magnitude is set at 0.45 arcsec to reduce the false candidate tally. Also, maximum point count, three or four, whichever applies is required.

4.2 Mixed epoch vectors

We have chosen to take residual differences between emulsions from the same epoch. That was influenced to

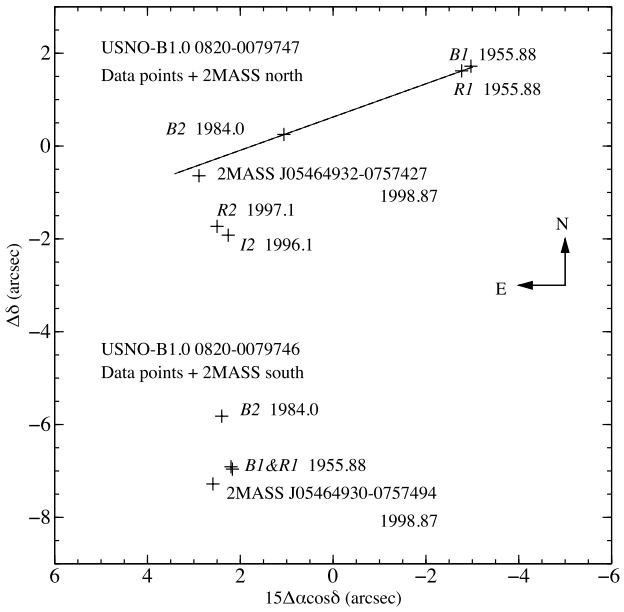

Figure 4. Plot in the observation epochs of data associated with 2MASS J05464932-0757427 and 2MASS J05464930-0757494. The origin is at the mean epoch for USNO-B1.0 0820-0079747, 1977.7, in the ICRS frame, with corrections obtained from GAVO (Roeser et al. 2010), $05^h46^m49^s.13$ -07°57′42″.1. A dashed line is drawn through the *B1, R1* and *B2* observations. The line indicates the object direction of travel with increasing time and is consistent with the position of 2MASS J05464932-0757427 at the time of its observation in 1998.87. The *R2* and *I2* observation positions are dislocated to the south as a result of inclusion in USNO-B1.0 0820-0079747 of the merged image of the northern and southern 2MASS stars at those times.

a great extent by difficulties with USNO-B pm values (Gould & Kollmeier 2004; Munn et al. 2004), as illustrated, for example, in Fig. 1b. For distant objects, which constitute the great majority of USNO-B entries, the pm is either zero or close to it and there is no good reason why vectors cannot be formed from differences in residuals between images from both epochs.

The introduction of vectors formed within and between epochs greatly increases the possibilities regarding combinations and numbers of vectors, but as long as each vector incorporates a blue observation the number of completely independent vectors will always be limited to two. Introducing mixed epoch vectors would allow analysis of entries that lack a *B2* observation and would be particularly effective with four observation entries that include both blue observations. The option of mixed epoch vectors merits notice, but will not be pursued further in this work.

5 PROBING USNO-B ENTRIES FOR CANDIDATE PAIRINGS AND GALAXIES

The exercise in Section 3 with sample groups of known quantities provided several insights germane to the more problematic task of probing the general population of USNO-B entries. The first step entails filtering out objects with unacceptable parameter values. Entries passing that gauntlet are then tested as described in the preceding sections and as amended below.

5.1 The candidate selection sieve

The initial set of filters includes:

(i) Eliminate all N=2 entries, all N=3 entries, except those with *B2, R2* and *I2* observations, and N=4 entries where *B2* is the missing quantity.

(ii) Eliminate all entries where any magnitude is 21 or dimmer. This step filters against false readings caused by artefacts such as emulsion defects.

(iii) Eliminate all entries where Δ magnitude $|B1\text{-}B2|>0.9$ and/or $|R1\text{-}R2|>0.9$. This requirement removes many of the hybrid entries and is slightly more exacting than the sample group requirement.

(iv) Include only entries in which $13<B2<19.5$ mag. This requirement guards against diffraction spikes on the low end and against inaccurate readings on the high end. It is a stringent requirement and on the high end, in and of itself, it eliminates a good fraction of all USNO-B entries.

(v) Avoid densely populated areas, generally, but not necessarily, in the Galactic equatorial plane. Several of the outliers in Section 3.2 experienced problems because of the passage of a neighbouring star. The density in the vicinities of those outliers was 8 objects arcmin^{-2} or greater. For this feasibility study we explore regions with densities <8 objects arcmin^{-2}. The average density of USNO-B entries over the celestial sphere is about 6.9 objects arcmin^{-2}, but the condition is restrictive due to the concentration about the Galactic plane.

Additionally, rooted on the experience of the test sample groups, we tighten the requirements for entries with five observations. An entry must comply with each of the following conditions for selection:

(i) All three displacement vectors must be greater than 0.35 arcsec.

(ii) Two of the three angle requirements between displacement vectors must be satisfied. That also puts a constraint on the third angle requirement.

(iii) $|\boldsymbol{I2\text{-}B2}|\text{-}|\boldsymbol{R2\text{-}B2}|> -0.15$ arcsec. This requirement combines and slightly modifies the three used with the sample groups.

Based on these revised requirements, the displacement vector requirement, in particular, several of the WD–dM sample group entries that had point count 6 would not now be selected. This step was none the less taken in an attempt to minimize false positives.

5.2 Candidates

Table 3 summarizes which areas of the celestial sphere have been sampled. The first column provides the central Galactic coordinates and the search area about that centre. The next column lists the number of USNO-B entries found in the sample area as acquired from VizieR. The following three columns provide the number of remaining entries after the filter at the column head has been activated, the value inclusive of all preceding filters. The next four columns indicate

Table 3. Summary of celestial sphere probes. See text for discussion of table content.

Galactic coord. centre (°)	Entries	Acceptable Obs.	Mag<21 diff.<0.9	13< *B2*<19.5	N=5	N=4 *R1+B1*	N=4 *R1* or *B1*	N=3 epoch 2	Density objs. arcmin^{-2}	
Window 40 arcmin per side										
0.0 +90.0	2335	887	515	174	2	0	1	0	1.5	
0.0 +60.0	5073	2275	1250	510	2	0	1	2	3.2	
120.0 +60.0	7669	2205	901	372	0	0	1	2	4.8	
240.0 +60.0	2733	1256	1197	423	3	1	3	2	1.7	
210.0 +45.0	2507	1145	872	405	0	0	1	0	1.6	
60.0 +30.0	6962	3775	2679	1579	8	0	0	0	4.4	
180.0 +30.0	5177	2493	1444	687	1	0	1	4	3.2	
210.0 +30.0	4246	2304	1831	740	5	1	1	0	2.7	
300.0 +30.0	9372	4431	3072	1583	1	0	7	1	5.9	
0.0 -90.0	3486	1365	678	331	0	0	1	5	2.2	
0.0 -60.0	3759	2131	2044	1068	0	0	18	1	2.4	
120.0 -60.0	3659	1407	913	337	1	0	0	1	2.3	
240.0 -60.0	3884	1592	983	524	0	0	8	0	2.4	
60.0 -30.0	6843	4280	3118	1790	6	1	8	1	4.3	
180.0 -30.0	3017	1533	1380	830	1	2	3	0	1.9	
300.0 -30.0	9204	5076	3501	2075	0	0	56	1	5.8	
Window 20 arcmin per side										
180.0 +0.0	2867	2059	1931	1053	11	2	2	0	7.2	
90.0-15.0	2803	2047	1841	990	4	2	0	1	7.0	
270+15	2600	1598	1391	920	0	0	9	2	6.5	Total objects of interest
15.0+15.0	3137	1985	1645	745	11	3	1	0	7.8	
Totals	91333	45844	33186	17136	56	12	122	23		213

the number of objects of interest for objects with five observations, four observations and a displacement vector in each of the epochs, four observations and epoch 2 displacement vectors, and three observations, both vectors in epoch 2. The final column gives the density of the initial entries arcmin^{-2}. The row at the bottom of the table sums each of the columns. The total number of objects of interest is 213. This number represents unscreened results. That is out of an initial 91,133 entries. The number of entries probed after filtering for acceptable observation detections and magnitudes is 17,136.

USNO-B images have been examined for all objects of interest. A total of 67 entries were removed from further consideration, overwhelmingly due to two problems: about two-thirds because of diffraction spikes from nearby bright objects and about one-third because of inconsistent object blending or separation from one emulsion to another. The removals were far from uniformly distributed. Of the 56 objects of interest with five observations 4 were removed. On the other hand, of the 122 items with four observations and two epoch 2 displacement vectors, 37 were removed. Further, of the 23 items with three observations and both displacement vectors in epoch 2, all 23 were withdrawn. Over half of those were phantom objects created out of the glare of the diffraction spikes. The diffraction spikes are consistently more prominent in the epoch 2 exposures than in those of epoch 1. Finally, of the 12 items with four observations and a displacement vector in each epoch, 3 were removed. These results highlight the robust nature of the entries with five observations. As for the relatively large number of items with four observations and two vectors in epoch 2, that can partly be attributed to the absence of any *B1* observations south of -33° declination. Table A3 provides a list of the 146 candidates remaining after screening. The first column furnishes the USNO-B identity, the next column the equatorial coordinates and the third column the number of observations. Succeeding columns list the displacement vector position angles and vector magnitudes. The final column notes USNO-B image characteristics and indicates availability of SDSS data.

6 SDSS DATA

6.1 WD–dM binary test set

Before considering SDSS data coincident with candidates in Table A3, we first return to the test set of WD–dM binaries, for which SDSS data is found for 30 of the 40 set members. Six of these members are flagged SATURATED, and are removed from consideration (see Stoughton et al. (2002) for a discussion of SDSS flagging). An additional six entries are flagged BLENDED, no deblend. That comes as no surprise, as blended objects are central to this study. However, interpreting the photometry of such objects is problematic. The SDSS telescopes have resolutions of about 1.5 arcsec, dependent upon seeing conditions. The pairs, flagged BLENDED, no deblend, have separations within the range of 0.655 to 2.0 arcsec. For one of these binaries, WD 0956+045, only

the dM is flagged. (Here, we again identify a binary by just one of its components, the WD).

The colour–colour plots of Figs. 5a and b display the remaining eighteen pairs and the unblended WD. Fig. 5a plots *g-r* versus *u-g* and Fig. 5b plots *r-i* versus *g-r*, where *u, g, r* and *i* are the ultraviolet, green, red and infrared SDSS bands. (*z* band data is not put to use here). The approximate locus for main-sequence stars is outlined on all diagrams (Richards et al. 2002; Smolčić et al. 2004; Covey et al. 2007). The WDs, with one exception, fall in the lower lefthand side of Fig. 5a and the dM in the upper righthand side, both as expected from a wide body of work (Lenz et al. 1998; Finlator et al. 2000; Smolčić et al. 2004; Covey et al. 2007; Rebassa-Mansergas et al. 2012, 2013). The exception is the DC white dwarf, WD 0725+827 (Silvestri et al. 2005). Cool WDs appear bluer than main-sequence stars at the same temperature (Silvestri et al. 2002) and from its position on the colour–colour plot the WD 0725+827 temperature is less than 5500°C. Six of the binaries, WD 0257-005, WD 1106+316, WD 1157+129, WD1236-004, WD1558+616 and WD 1833+644, have been identified as a single star by SDSS, and lie within the WD region. Five of these binaries have separations ranging from 0.478 to 0.72 arcsec, which in this case was close enough to elude detection of blending. The sixth binary, WD 1833+644 is a multiple with separations of 0.079 and 1.82 arcsec. The nearer companion is 4 magnitudes brighter than the farther one (Farihi et al. 2010).

Only a few dMs are plotted on Fig. 5a. The others exceed 20.5 mag in the *u* band. At less than 20.5 mag the accuracy of the *u* band measurements is better than 0.1 mag (Smolčić et al. 2004). [At 22 mag, the limiting signal-to-noise level is 5:1 (Ivezić et al. 2000), good enough for detection, but not for accurate photometry]. Eleven dMs are plotted in Fig 5b. (One dM is too faint in the *g* band to be plotted). Note that only WD 0725+827 is identified on Fig. 5a. No individual stars are identified on Fig. 5b.

6.2 Candidates coincident with SDSS data

SDSS observations coincide with 37 of the candidate entries. Two of these observations have a SATURATION flag and one an EDGE flag. The remaining entries are listed in Table 4, representing a little less than a quarter of the total number of candidates. Table 4 is divided into two parts, the first for single objects in which one SDSS item coincides with the USNO-B entry and the second part for paired objects in which SDSS has resolved or deblended two entities. The first column of Table 4 numbers the entry for easy identification on Fig. 5. That is succeeded by the USNO-B and SDSS identifications and by a column designating a galaxy as indicated by SDSS. The following columns list the values of *u*, *u-g*, *g-r*, and *r-i*. For those objects designated as galaxies by SDSS the values of *u-g* and *g-r*, corrected for reddening, as determined by Schlafly & Finkbeiner (2011), are parenthetically indicated adjacent to the uncorrected values. Their work has used SDSS data to improve upon the maps previously developed by Schlegel, Finkbeiner & Davis (1998). Corrections have not been applied to *r-i* or to stellar objects. Judging from the galactic results at the shorter wavelengths, such corrections for colour differences would not exceed 0.075 mag and their absence does not affect our conclusions. A second row in the paired object section records the same information for the second SDSS object. The next two columns provide computed separation and position angles for the paired SDSS entries and the final column assesses the apparent nature of the object as determined from the SDSS designation and from the colour–colour diagrams of Fig. 5.

6.2.1 *Single objects*

The single objects include the first ten entries of Table 4 and additionally two entries from the second portion of the table, #'s 12 & 18, whose companions are too faint in all bands to have influenced USNO-B selection. Both of those entries are identified as galaxies, for a total of seven of the twelve single objects designated as galaxies by SDSS . Two of those objects are flagged BLENDED, no deblend. Regarding galaxy selection, our methodology works with distant systems. Galaxies that subtend tens of arc-seconds and more are either perceived by USNO-B as extremely bright objects (USNO-B magnitude evaluation depends upon image diameter) or are often apprehended as a series of smaller objects. In the first instance bright magnitude filtering eliminates the entry and in the second, should the object make its way through filtering and analysis, it then should be eliminated on visual inspection. The two galaxies flagged BLENDED, no deblend, are not nearby, their images span only a few arc-seconds, but they none the less fall into the latter category and eluded being discarded in the initial visual inspection. The other five galaxies appear as small images. Entry #12 is plotted on Fig. 5c and falls close to the separator line between red and blue galaxies (dashed line, from Strateva et al. (2001)). That is suggestive of a bi-coloured galaxy, but the significance of the selection of this galaxy, as well as the other four, requires observational input. Strateva et al. (2001) selected a population of galaxies with a cutoff of $g<22$ mag. Entry #12 satisfies that condition, but the *u* band accuracy is probably no better than 0.2 mag.

Of the remaining five single object entries two, #'s 6 and 7, have faint *u* and *g* magnitudes and each has four USNO-B observations, i.e., two displacement vectors, both dependent upon *B2*. Although USNO-B *B2* is less than 19.5 mag for both, that is at considerable variance with the SDSS data and no attempt is made to further identify these two entries. Object #'s 4, 9 and 10 fall within the main-sequence locus. The significance of their selection, again, requires more specific observational data.

6.2.2 *Paired objects*

The salient point for the paired object portion of Table 4 revolves about a comparison between the position angle of the two SDSS components and the average position angle of the corresponding USNO-B displacement vectors (see Table A3 for displacement vector data). Out of a total of 22 items we find the following:

Fifteen entries agree within 9°, ten of those within 5°.
Six entries agree within a range of 11°– 24°.

The remaining entry, #17, USNO-B 0984-0266003, deviates from alignment by 31°. The separations for the 22

Table 4. USNO-B1.0 entries coincident with SDSS data. Tentative identifications are indexed as follows: (1) galaxy; (2) resolved WD–dM; (3) compact WD–dM paired with main-sequence star; (4) galaxy paired with faint object; (5) main-sequence star paired with apparent red giant; (6) galaxy BLENDED, no deblend; (7) galaxy paired with main-sequence star; (8) two main-sequence stars paired; (9) main-sequence star. See text and Fig. 5 for a more detailed description.

#	USNO-B1.0	SDSS	s/g	u (mag)	u-g (mag)	g-r (mag)	r-i (mag)	sep. (arcsec)	PA (°)	Tentative Identity
1	0924-0009909	J004422.53+022948.9	galaxy	20.317	0.775 (0.758)	0.699 (0.682)	0.324			(1)
2	0970-0663419	J212814.67+070050.4	galaxy	21.439	1.780 (1.717)	1.314 (1.245)	0.512			(1)
3	0971-0681235	J212726.08+071006.0	galaxy	20.604	1.042 (0.980)	0.703 (0.635)	0.357			(1)
4	0972-0698506	J212829.26+071614.2		20.077	1.695	0.671	0.217			(9)
5	1006-0190377	J110311.18+103932.2	galaxy/BLD							(6)
6	1006-0190380	J110313.16+103753.1		25.035	3.480	1.266	0.658			
7	1009-0190583	J110305.90+105657.0		23.100	1.810	1.529	0.789			
8	1010-0189647	J110317.05+110218.9	galaxy	22.256	0.991 (0.970)	1.576 (1.553)	0.748			(1)
9	1010-0189899	J110457.60+110150.0		18.927	1.219	0.505	0.209			(9)
10	1170-0240143	J125034.32+270059.1		20.722	1.039	0.574	0.217			(9)
11	0966-0584913	J212750.95+063951.7		21.409	0.866	0.668	0.136	4.6	129	(8)
		J212751.19+063948.8		19.535	1.491	0.551	0.187			
12	0969-0633655	J212736.77+065924.5	galaxy	21.333	1.149 (1.087)	0.867 (0.800)	0.401			(4)
		J212736.59+065928.2		24.484	0.911	0.491	-0.582			
13	0969-0633980	J212826.21+065837.3		19.344	1.552	0.581	0.247	3.0	90	(8)
		J212826.41+065837.3		21.043	2.617	1.383	0.645			
14	0969-0634114	J212851.73+065748.3	galaxy	21.260	1.505 (1.439)	0.288 (0.215)	0.122	2.1	203	(7)
		J212851.70+065746.3		22.275	1.947	1.050	0.324			
15	0971-0681479	J212802.37+071015.8		23.098	3.226	1.341	0.578	4.7	280	
		J212802.68+071016.6	star/BLD	21.777[a]	-0.030[a]	0.089[a]	-0.386[a]			
16	0971-0681705	J212836.71+070849.8	galaxy	22.173	1.888 (1.822)	1.449 (1.377)	0.504	4.5	13	(7)
		J212836.64+070845.4		20.234	1.237	0.490	0.149			
17	0984-0266003	J143154.01+082559.3		19.455	2.464	1.080	0.401	5.4	233	(7)
		J143154.30+082602.6	galaxy	21.153	0.939 (0.918)	0.229 (0.206)	0.151			
18	1009-0190822	J110435.73+105746.1	galaxy/BLD							(4), (6)
		J110435.40+105740.7		23.214	1.325	1.192	0.512			
19	1053-0170335	J083536.69+151945.9		19.420	2.520	1.339	0.616	4.7	143	(8)
		J083536.49+151949.7		17.743	1.303	0.483	0.163			
20	1053-0170642	J083647.69+152210.7		19.089	2.081	0.820	0.316	3.7	262	(2)
		J083647.94+152211.2		20.923	1.096	-0.232	-0.095			
21	1054-0169679	J083539.07+152536.8		21.182	0.982	0.395	0.200	6.5	136	(8)
		J083539.38+152532.1		16.467	1.289	0.458	0.119			
22	1055-0172337	J083722.27+153038.0		18.788	1.519	0.559	0.188	5.3	154	(8)
		J083722.43+153033.2		21.151	2.397	1.317	1.206			
23	1058-0172600	J083625.35+155111.5		17.996	1.389	0.494	0.157	5.6	208	(8)
		J083625.17+155106.6		24.149	2.859	1.526	1.365			
24	1058-0172658	J083650.62+154859.0		16.809	1.054	0.160	0.015	5.1	246	(8)
		J083650.30+154856.9		23.580	3.175	1.570	0.934			
25	1108-0181990	J093344.32+205300.1		22.479	2.700	1.436	0.904	4.9	268	(7)
		J093344.67+205300.3	galaxy	21.659	1.084 (1.056)	0.744 (0.713)	0.311			
26	1169-0233621	J125133.53+265508.6		19.217	0.991	0.292	0.129	4.4	245	(8)
		J125133.23+265506.7		25.542	2.661	1.546	1.659			
27	1189-0098459	J054534.11+285958.2		21.623	1.894	1.144	0.602	3.5	262	(8)
		J054533.85+285957.7		24.901	3.602	1.370	0.756			
28	1190-0098093	J054521.60+290533.1		19.489	1.810	0.974	0.472	7.75	79	(3)
		J054521.02+290531.6		16.586	1.356	0.634	0.181			
29	1190-0098147	J054526.89+290542.8		19.154	1.991	0.753	0.383	4.1	274	(8)
		J054526.58+290543.1		23.237	3.727	1.758	0.889			
30	1190-0098184	J054530.59+290507.8		19.533	1.726	0.926	0.450	4.2	169	(3)
		J054530.65+290503.7		22.668	2.506	1.561	1.239			
31	1251-0258748	J173339.42+351123.4		19.092	0.183	-0.374	-0.322	2.3	141	(2)
		J173339.54+351121.6		25.321	4.769	1.293	1.066			
32	1252-0258837	J173435.38+351725.6		20.836	1.567	0.545	0.265	7.2	290	(6), (7)
		J173435.93+351723.1	galaxy/BLD							
33	1253-0259828	J173420.48+351941.1		19.498	1.023	0.284	0.010	1.8	251	(5)
		J173420.34+351940.5		24.540	3.055	2.213	1.463			
34	1254-0260615	J173414.57+352745.0		19.848	1.248	0.471	0.158	2.7	281	(8)
		J173414.35+352745.5		25.108	4.575	1.381	0.690			

Note [a] Although the second component of object #15 is flagged BLENDED, no deblend, the photometry is retained as discussed in the text.

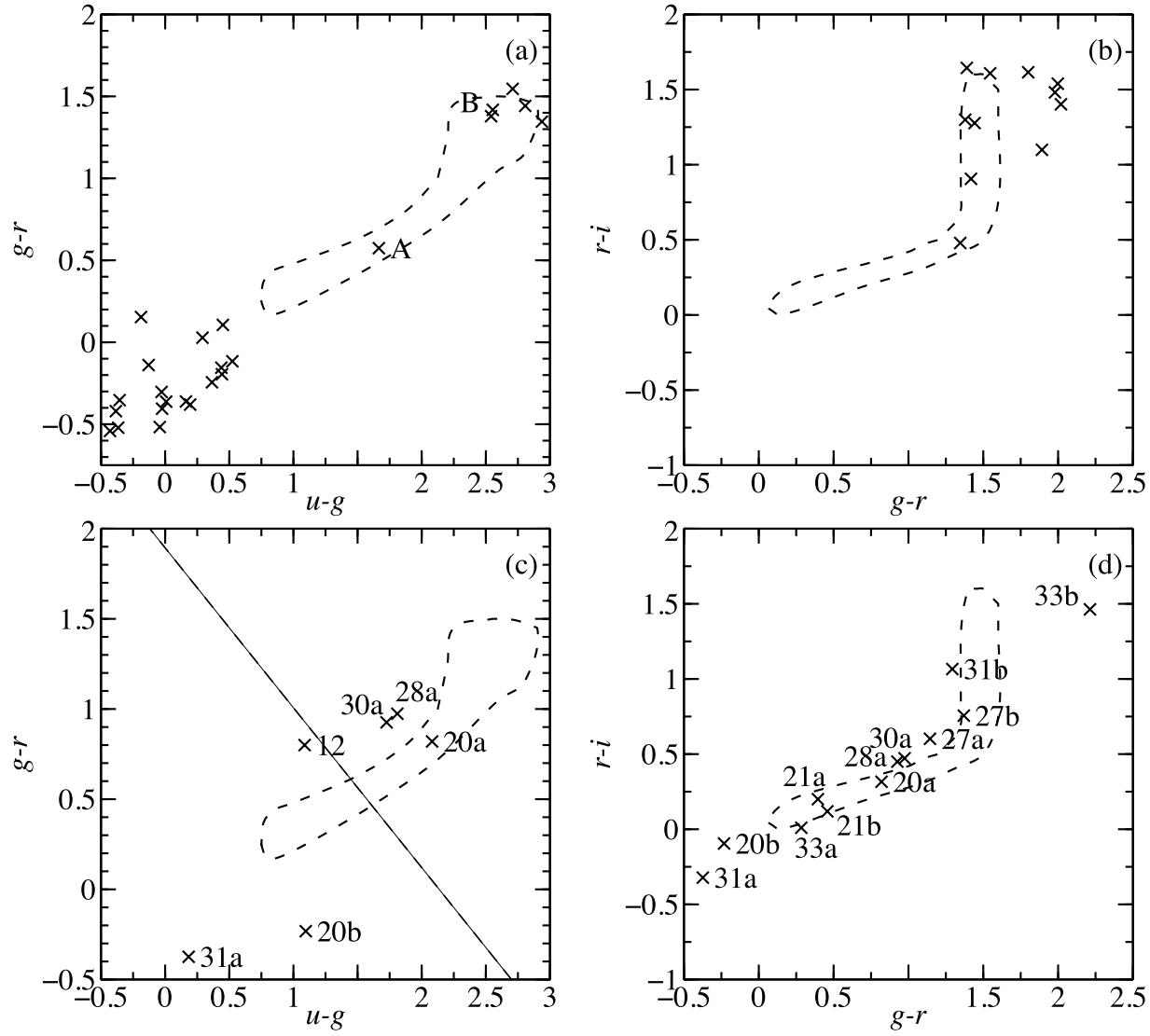

Figure 5. Colour–colour plots of WD–dM sample set pairs and of USNO-B1.0 candidate objects employing SDSS data. Fig. 5a depicts WDs (lower left) from the WD–dM sample set and a few of their dM companions (upper right). WD 0725+827 ('A') and its dM companion, LP 5-74 ('B') are the only two stars identified on the plot. Most of the dM companions are plotted in Fig. 5b. See Section 6.2 for a discussion of objects plotted in Figs. 5c and 5d.

entries range from 1.8–7.75 arcsec, in accord with expectations.

Turning to the tentative identification of the entries, colour difference analysis, i.e., *g-r* versus *u-g* and *r-i* versus *g-r*, plus SDSS star/galaxy discrimination leads to the following conclusions:

(i) Eleven entries are main-sequence pairs, eight of them an dM paired with an earlier star. All eleven pairs exhibit extended USNO-B images. Both components of two of the exceptions, #'s 21 & 27, USNO-B 1054-0169679 and USNO-B 1189-0098459, are plotted on Fig. 5d. The close delta spectral spacings is of interest here. The spatial separations of the components, from Table 4, are 6.5 and 3.5 arcsec, respectively. To limit congestion, the third exception, # 11, USNO-B 0966-0584913, was not plotted, but it is similarly closely spaced spectrally. Its components are spatially separated by 4.6 arcsec.

(ii) Two entries appear to be resolved WD–main-sequence pairs, one of them a WD–dM. Both pairs, #'s 20 and 31, USNO-B 1053-0170642 and USNO-B 1251-0258748, are plotted in Fig. 5d. Pair # 20 is also plotted in Fig. 5c, along with the WD component of pair # 31. A third pair, entry #15, has a star flagged BLENDED, no deblend and is not plotted. We have retained the photometry in Table 4, which, would place it in the WD region. Regardless of blending, it is difficult to envisage the object being in this region without it having a blue component. Its luminous output is virtually flat over the *u, g* and *r* bands, indicative of a high temperature. Despite a faint output of about 21.8 mag, USNO-B 2nd epoch blue exposures show an extended object, aligned as per the position angles of Table A3. The average position angle alignment is within 14° of that of the SDSS pair.

(iii) Two entries are possibly unresolved WD–dM binaries, as per Smolčić et al. (2004), paired with main-sequence stars, although they are marginally in the WD–dM region

and may in fact be main-sequence pairs. The apparent WD–dM components of both of these objects, #'s 28a and 30a are plotted in Figs. 5c & d.

(iv) Five entries are galaxies paired with main-sequence stars, one of the galaxies flagged, BLENDED, no deblend.

(v) One entry may be an M giant/carbon paired with a main-sequence star as per Covey et al. (2007). However, this designation is speculative and is based on its distance from the main-sequence locus. Several of the dMs from the sample set, plotted in 5b are similarly outside of the locus, although not as wide. Both components are plotted in Fig. 5d. This entry, #33, USNO-B 1253-0259828, and one of the apparent WD–dM pairs, #31, USNO-B 1251-0258748, exhibit the widest spectral separations.

6.3 Discussion of SDSS results

We emphasize that the identity of objects in Table 4 is tentative. The sample set provided an illustration of how a cool WD, falling well within the colour–colour main-sequence locus could easily be misidentified.

Our designation of two pairs as WD–dM compact binaries paired with main-sequence stars is open to question, as is the tentative identification of one pair as an M giant/carbon star paired with a main-sequence star. It may well be that we have selected fourteen main-sequence binaries rather than eleven. On the other hand the identification of two objects as WD–main-sequence pairings, and a possible third, appears to be credible. Though main-sequence pairs with extended USNO-B images were expected to be uncovered, the detection of three pairs closely spaced on the colour–colour plots is not easily explained. In all three instances one component is brighter than the other in all bands.

The alignment of all SDSS paired objects with the corresponding USNO-B displacement vector position angles stands out as the prime result of this exercise, and it goes a long way towards affirming our central premise regarding the detection of objects with displaced blue and red components. Though we have been clear throughout this paper in our preference for USNO-B entries with five observations as contrasted with those with four, we point out that eight of those aligned paired objects were entries with four observations.

7 CONCLUSIONS

This feasibility study aimed at demonstrating the value of the USNO-B1.0 catalogue for selecting objects with displaced blue and red components. The specifics of the approach were developed with the aid of analysis of three sample test sets of known properties. Over 91,000 USNO-B entries were then sifted and analysed and the results visually screened to obtain a candidate list of 146 objects. Slightly less than a quarter of this list coincided with SDSS data, which was used for tentative identification of object types and, most importantly, confirmed that displacement vectors formed from the USNO-B data aligned with corresponding SDSS pair position angles.

That confirmation leads us to reexamine restrictions that were added after the test set analysis. In particular, USNO-B five observation entries were required to have all displacement vector magnitudes greater than 0.35 arcsec and four observation entries were required to have vector magnitudes greater than 0.45 arcsec. Relaxation of these strictures to lower thresholds would lead to a greater number of candidates and improved sensitivity at shorter pair separation distances. Too great a relaxation will result in large numbers of false positives. We expect that values of 0.3 arcsec for five observation entries, and 0.4 arcsec for four observation entries would be suitable.

Another restriction that bears reevaluation is the maximum acceptable magnitude for *B2*, which was set at 19.5 mag. There was good reason for this restriction, especially for four observation entries, due to the dependence of two vectors on *B2* and hence an interdependence between the two that is especially damaging for the errant values of *B2* more likely to occur at faint magnitudes. However, this constraint was one of the most limiting with regard to reducing the number of entries suitable for analysis. For those who would make use of this procedure, and specifically at the higher galactic latitudes, raising the ceiling to 20 mag is worthy of exploration. Our overwhelmingly negative result with three observation entries leads us to conclude that it is unproductive to pursue this course any further, though conceding that this conclusion is based on a small sample. What would be worthwhile is the introduction of mixed epoch vectors (see Section 4.2), which would expand the number of entries open to analysis.

Although we have established the effectiveness of our approach in selecting objects with displaced coloration there is still the question of its usefulness. Those studying low mass ratio main-sequence binaries might find the efficiency marginal, and those seeking WD binaries would hardly be tempted by the low yield. And while we have clear evidence regarding the detection of WD and main-sequence pairs, our suppositions regarding the types of single object galaxies detected remains speculative until confirmed, or otherwise, by observation. It seems clear that mounting an effective programme to exploit this tool would require a collaborative effort in which the different components of the team would have diverse interests. The motivation for such an effort assuredly lies in the expanse of USNO-B. This study has explored segments of the catalogue that, in total, encompass less than 0.01 per cent of that expanse.

ACKNOWLEDGEMENTS

The author thanks David G. Monet for providing a copy of the USNO-B1.0 survey logs. He further thanks the referee, Dimitri Pourbaix, for his constructive comments and suggestions.

This research has made extensive use of the USNO Image and Catalogue Archive operated by the United States Naval Observatory, Flagstaff Station (http://www.nofs.navy.mil/data/fchpix/). Substantial use has also been made of the Simbad data base and the VizieR catalogue access tool, CDS, Strasbourg, France. The original description of the Simbad and VizieR services were published, respectively, in A & AS, 2000, 143, 9 and 23.

Funding for SDSS-III has been provided by the Alfred P. Sloan Foundation, the Participating Institutions,

the National Science Foundation, and the U.S. Department of Energy Office of Science. The SDSS-III web site is http://www.sdss3.org/ .

SDSS-III is managed by the Astrophysical Research Consortium for the Participating Institutions of the SDSS-III Collaboration including the University of Arizona, the Brazilian Participation Group, Brookhaven National Laboratory, Carnegie Mellon University, University of Florida, the French Participation Group, the German Participation Group, Harvard University, the Instituto de Astrofisica de Canarias, the Michigan State/Notre Dame/JINA Participation Group, John Hopkins University, Lawrence Berkeley National Laboratory, Max Planck Institute for Astrophysics, Max Planck Institute for Extraterrestrial Physics, New Mexico University, New York University, Ohio State University, Pennsylvania State University, University of Portsmouth, Princeton University, the Spanish Participation Group, University of Tokyo, University of Utah, Vanderbilt University, University of Virginia, University of Washington, and Yale University.

REFERENCES

Abazajian K. N. et al., 2003, AJ, 126, 2081
Ahn C. P. et al., 2012, ApJS, 203, 21
Bailey J.,1998, MNRAS,301, 161
Christy J.W, Wellnitz D.D., Currie D.G., 1983, Lowell Observatory Bulletin, 167, 28
Clarke C.J., 2009, MNRAS, 396, 1066
Covey K.R. et al., 2007, AJ, 134, 2398
Duchêne G., Kraus A., 2013, ARA&A, 51, 269
Farihi J., Hoard D.W., Wachter S., 2006, ApJ, 646, 480
Farihi J., Hoard D.W., Wachter S., 2010, ApJS, 190, 275
Finlator K. et al., 2000, AJ, 120, 2615
Fischer D.A., Marcy G.W., 1992, ApJ, 396, 178
Forgan D., Rice K., 2011, MNRAS, 417, 1928
Gould A., Kollmeier J.A., 2004, ApJS, 152, 103
Hoard D.W., Wachter S., Sturch L.K., Widhalm A.M., Weiler K.P., Pretorius M.L., Wellhouse J.W., Gibiansky M., 2007, AJ, 134, 26
Høg E. et al., 2000, A&A, 355, L27
Ivezić Z. et al., 2000, AJ, 120, 963
Janson M. et al., 2012, ApJ, 754, 44
Janson M., Bergfors C.,Brandner W., Kudryavtseva N., Hormuth F., Hippler S., Henning T., 2014, ApJ, 789, 102
King I. R., Raff M. I., 1977, PASP, 89, 120
Kleinman S.J., et al., 2013, ApJ, 204, 5
Lenz D.D., Newberg H.J., Rosner R., Richards G.T., Stoughton C., 1998, AJ, 119, 121
Li L.F., Gong X.B., Zhang F.H., Han, Q.W., Kong X.Y., 2014, MNRAS, 445, 1331
McCook G.P., Scion, E.M., 1999, ApJS, 121, 1
Minkowski R.L., Abell G.O., in 'Basic Astronomical Data' edited by Strand, K. Aa, U. Chicago Press, Chicago, 1963, p. 481
Monet D. G. et al., 2003, AJ, 125, 984
Montagnier G. et al., 2006, A&A, 460, L19
Munn J.A., Monet D.G., Levine S.E., Canzian B., Pier J.R., Harris H.C., 2004, AJ, 127, 3034
Pourbaix D., Ivesić Ž., Knapp G.R., Gunn J.E., Lupton R.H., 2004, A&A, 423, 755
Rebassa-Mansergas A., Nebot Gomez-Morain A., Schreiber M.R., Gansicke B.T., Schwope A., Gallardo J., Koester D., 2012, MNRAS, 419, 806
Rebassa-Mansergas, A., Agurto-Gangas C., Schreiber M.R., Gansicke B.T., Koester D., 2013, MNRAS, 433, 3398
Reggiani M., Meyer M.R., 2013, A&A, 553, A124
Richards G.T., et al., 2002, AJ, 123, 2945
Roeser S., Demleitner M., Schilbach E., 2010, AJ, 139, 2440
Schlafly E.F., Finkbeiner D P., 2011, ApJ, 737,103
Schlegel D. J., Finkbeiner D. P., Davis M., 1998, ApJ, 500, 525
Silvestri N.M., Oswalt T.D., Hawley S.L., 2002, AJ, 124, 1118
Silvestri N.M., Hawley S.L., Oswalt T.D., 2005, AJ, 129, 2428
Skrutskie M.F. et al., 2006, AJ, 131, 1163
Smolčić V. et al., 2004, ApJ, 615, L141
Sorokin L.Y., Tokovinin A.A., 1985, SvAL, 11, 226
Stoughton C. et al., 2002, AJ, 123, 485
Strateva I. et al., 2001, AJ, 122, 1861
Wielen R., 1996, A& A, 314, 679
York D. G., et al., 2000, AJ, 120, 1579

APPENDIX A: TABLES A1, A2, A3

This paper has been typeset from a TEX/LATEX file prepared by the author.

Table A1. Single star sample set. Coordinates are in equinox J2000, epoch J2000.

USNO-B1.0 id.	Alt. id.	RA ($^h\ ^m\ ^s.$)	Dec ($^\circ\ '\ ''.$)	r_{rms}	pts.
0824-0001341	GJ 1002	00 06 43.13	-07 32 16.87	0.14	2
1192-0001921	GJ 1003	00 07 26.70	+29 14 32.80	0.09	2
0833-0006357	GJ 1012	00 28 39.46	-06 39 49.08	0.11	0
0841-0005187	GJ 1013	00 31 35.40	-05 52 12.99	0.19	2
0855-0009698	GJ 1025	01 00 56.37	-04 26 56.33	0.15	1
1523-0040804	GJ 51	01 03 19.87	+62 21 55.93	0.13	4
0611-0011923	GJ 1031	01 08 18.28	-28 48 20.09	0.13	2
0654-0012495	GJ 2021	01 09 18.71	-24 30 23.49	0.15	3
0949-0011332	GJ 3078	01 11 57.99	+04 54 12.57	0.07	0
0838-0017238	GJ 3119	01 51 04.10	-06 07 05.15	0.12	4
0811-0020420	LP709-43	02 10 03.65	-08 52 59.62	0.20	3
0860-0020514	LHS 1363	02 14 12.58	-03 57 43.54	0.20	0
1068-0028941	GAT 1370	02 53 00.88	+16 52 52.76	0.12	2
0696-0041248	LHS 1491	03 04 04.48	-20 22 43.23	0.19	3
0592-0035569	LP888-18	03 31 30.24	-30 42 38.81	0.28	5
0839-0036868	GJ 1065	03 50 44.31	-06 05 41.61	0.12	0
1070-0040309	GJ 3253	03 52 41.75	+17 01 04.19	0.12	4
0655-0044012	LHS 1630	04 07 20.48	-24 29 13.53	0.07	1
0953-0073703	GJ 1087	05 56 25.47	+05 21 48.57	0.13	2
1134-0116117	GJ 232	06 24 41.28	+23 25 59.08	0.13	5
1523-0188659	GJ 3417	06 57 57.13	+62 19 19.54	0.16	3
1427-0213945	GJ 3421	07 03 55.76	+52 42 06.89	0.22	2
1494-0183213	GJ 3512	08 41 20.12	+59 29 50.72	0.17	1
0865-0193882	GJ 3517	08 53 36.18	-03 29 32.29	0.22	3
1383-0239712	GJ 1151	11 50 57.74	+48 22 38.77	0.18	5
0662-0267348	Note 1	12 14 08.71	-23 45 16.79	0.14	2
0906-0208882	GJ 1154	12 14 16.56	+00 37 26.47	0.16	3
0956-0217859	GJ 493.1	13 00 33.54	+05 41 08.21	0.13	0
1497-0221149	GJ 3855	14 30 37.79	+59 43 25.15	0.13	2
1308-0269841	GJ 3959	16 31 18.79	+40 51 51.93	0.07	0
1124-0308674	GJ 3976	16 50 57.95	+22 27 05.68	0.09	1
0856-0301315	GJ 1207	16 57 05.72	-04 20 56.64	0.10	-1
1414-0271453	GJ 3988	17 03 23.90	+51 24 23.03	0.12	3
1608-0117171	GJ 1221	17 48 00.00	+70 52 36.17	0.16	4
1542-0210205	G 227-22	18 02 16.63	+64 15 44.62	0.08	1
1520-0275071	GJ 1227	18 22 27.14	+62 03 01.95	0.22	3
1054-0588142	GJ 1256	20 40 33.86	+15 29 58.89	0.13	3
0723-1162500	GJ 4274	22 23 06.99	-17 36 26.29	0.13	1
1341-0523884	GJ 905	23 41 55.04	+44 10 39.07	0.17	1
0738-0841136	GJ 4360	23 45 31.25	-16 10 20.07	0.10	1

Note 1. Alternate identification is 2MASS J12140866-2345172

Table A2. Binary sample sets. Coordinates are in equinox J2000, epoch J2000. For both sets of data only one component of the binary is listed under 'Alternate ident.' The references for the dM binary set are Janson et al. (2012, 2014). References for the WD–dM binary set (in parentheses after separation) are: (1) Hoard et al. (2007), (2) Silvestri, Hawley & Oswalt (2005) and (3) Farihi et al. (2006, 2010). 'WDS' indicates that the separation was obtained from the USNO Washington Double Star Catalogue. The SDSS column indicates whether or not (Y or blank) SDSS data is available for the WD–dM binary entry (see Section 6.1.

USNO-B1.0 ident.	Alternate ident.	RA (^{h} ^{m} ^{s}.)	Dec ($^\circ$ $'$ $''$.)	Separation (arcsec)	SDSS (WD–dM)	Point count
		dM binary sample set				
	2MASS					
0854-0005123	J00325313-0434068	00 32 53.13	-04 34 06.9	0.42-0.51		1
1308-0018556	J01034210+4041158	01 03 42.11	+40 51 16.1	1.5-2.5		2
0823-0016981	J01132958-0738088	01 13 29.59	-07 38 08.8	2.9		3
0832-0024712	J01365516-0647379	01 36 55.18	-06 47 38.5	5.4		1
0750-0018344	J01535076-1459503	01 53 50.76	-14 59 50.2	2.8		3
0805-0022317	J02155892-0929121	02 15 58.93	-09 29 12.0	0.06/3.4		4
0666-0026418	J02165488-2322133	02 16 54.80	-23 22 12.0	4.3		0
0605-0025977	J02271603-2929263	02 27 16.04	-29 29 26.2	1.9		3
0883-0068712	J04132663-0139211	04 13 26.62	-01 39 21.2	0.74		3
0663-0056479	J05100488-2340148	05 10 04.88	-23 40 14.9	1.8		2
0890-0056913	J05191382-0059423	05 19 13.80	-00 59 43.7	1.1		5
0573-0081113	J05344858-3239362	05 34 48.59	-32 39 36.3	2.1/0.44		0
0848-0062045	J05350429-0508125	05 35 04.48	-05 08 13.3	4.1		2
0820-0079747	J05464932-0757427	05 46 49.34	-07 57 44.2	2.8		4
0780-0096591	J05494272-1158500	05 49 42.60	-11 58 49.7	3.4		0
0780-0096591	J06281861-0110504	06 28 18.59	-01 10 50.7	1.4		5
1377-0208428	J06351837+4745366	06 35 18.64	+47 45 37.2	3.5∼3.9		2
0696-0115277	J06583980-2021526	06 58 39.76	-20 21 52.9	1.4		4
1344-0192252	J07505369+4428181	07 50 53.69	+44 28 18.5	2.0		1
1302-0190151	J08310177+4012115	08 31 01.78	+40 12 11.8	1.9		2
0761-0200741	J08483645-1353083	08 48 36.72	-13 53 07.7	7.4/0.3		5
0591-0203730	J08540240-3051366	08 54 02.38	-30 51 36.7	1.7		2
0885-0192790	J10122171-0128160	10 12 21.68	-01 28 15.9	2.9		2
1053-0192207	J10364483+1521394	10 36 44.84	+15 21 39.3	0.17/1.0		0
1216-0196987	J11281625+3136017	11 28 16.24	+31 36 01.8	1.1		1
0786-0233601	J12134173-1122405	12 13 41.73	-11 22 40.9	1.3		3
1326-0292758	J13015919+4241160	13 01 59.17	+42 41 16.3	2.9		1
1222-0276082	J13120525+3213332	13 12 05.30	+32 13 33.5	0.9		0
1548-0176179	J14190331+6451463	14 19 03.32	+64 51 46.7	4.6		2
1035-0224299	J14360274+1334484	14 36 02.73	+13 34 48.6	1.2		1
1341-0273828	J14450627+4409393	14 45 06.29	+44 09 39.2	5.2		2
0893-0244088	J15032251-0040310	15 03 22.65	-00 40 30.9	3.8		1
1252-0234146	J15553178+3512028	15 55 31.80	+35 12 02.7	1.5-1.6		4
1340-0271823	J15594729+4403595	15 59 47.31	+44 03 59.9	5.6		4
1538-0209444	J16363309+6353452	16 36 33.05	+63 53 44.9	0.2/3.4		2
1317-0302575	J16460779+4142057	16 46 07.73	+41 42 07.4	5.7		4
1259-0251199	J16510995+3555071	16 51 09.97	+35 55 07.2	1.0		2
1023-0718446	J21035992+1218570	21 03 59.93	+12 18 57.0	0.83		-1
0817-0690783	J21091375-0814041	21 09 13.74	-08 14 03.9	0.97		1
0803-0681472	J22332264-0936537	22 33 22.65	-09 36 53.5	1.5		2

Table A2 – *continued* binaries

USNO-B1.0 ident.	Alternate ident.	RA (^{h} ^{m} ^{s}.)	Dec ($^\circ$ $'$ $''$.)	Sep. (Ref.) (arcsec)	SDSS (WD–dM)	Point count
			WD–dM binary sample set			
	WD ident.			Sep. (Ref.)		
1000-0002069	WD 0014+097	00 16 56.15	+10 03 58.8	<4 (1)	Y	6
0742-0019772	WD 0158-160	02 00 56.69	-15 46 10.7	5.7-7.8/WDS (2)	Y	1
1036-0021298	WD 0205+133	02 08 03.49	+13 36 25.1	1.257 (3)	Y	7
1277-0045811	WD 0217+375	02 20 25.25	+37 47 30.9	∼2 (2)		2
0896-0030878	WD 0257-005	03 00 24.56	-00 23 41.8	0.978 (3)	Y	4
1549-0145856	WD 0911+651	09 15 32.05	+64 56 41.2	6 (2)	Y	5
1098-0172007	WD 0915+201	09 18 33.04	+19 53 07.8	2.312 (3)	Y	6
0923-0231599	WD 0933+025	09 35 40.70	+02 22 00.2	1.232 (3)	Y	6
1349-0213613	WD 0949+451	09 52 22.00	+44 54 29.8	2.892 (3)	Y	5
1083-0198558	WD 0950+185	09 52 45.80	+18 21 03.1	1.1 (1)	Y	7
0943-0177699	WD 0956+045	09 58 37.25	+04 21 31.0	2 (1)	Y	4
0941-0190204	WD 1104+044	11 07 04.76	+04 09 09.2	∼3 (2)	Y	7
1213-0187197	WD 1106+316	11 08 43.05	+31 23 56.2	0.478 (3)	Y	2
1086-0195362	WD 1123+189	11 26 19.09	+18 39 17.2	1.3 (1)	Y	5
1026-0245938	WD 1157+129	11 59 15.65	+12 39 30.0	0.564 (3)	Y	3
1361-0222911	WD 1210+464	12 12 59.64	+46 09 47.0	1.043 (3)	Y	7
0929-0275178	WD 1214+032	12 16 51.86	+02 58 04.7	2 (1)	Y	6
1220-0233210	WD 1215+322	12 17 33.26	+32 05 09.0	6.6-7/WDS (2)	Y	4
0893-0216590	WD 1236-004	12 38 36.34	-00 40 42.2	0.658 (3)	Y	4
1651-0066694	WD 1240+754	12 42 03.85	+75 08 43.8	6 (2)		5
0755-0271141	WD 1307-141	13 10 22.53	-14 27 09.1	2.133 (3)		7
1384-0238519	WD 1333+487	13 36 01.95	-48 28 46.7	2.947 (3)	Y	6
1403-0256955	WD 1402+506	14 04 08.95	+50 20 38.4	5 (2)	Y	6
1474-0288101	WD 1419+576	14 21 05.37	+57 24 57.4	0.655 (3)	Y	4
1268-0246415	WD 1435+370	14 37 36.71	+36 51 37.5	1.251 (3)	Y	6
0591-0203730	WD 1443+337	14 46 00.72	+33 28 50.1	0.679 (3)	Y	6
1247-0222694	WD 1502+349	15 04 31.86	+34 47 00.0	1.913 (3)	Y	5
0760-0301587	WD 1539-137	15 42 00.94	-13 56 06.6	∼7 (2)		5
1515-0219383	WD 1558+616	15 58 55.55	+61 32 03.8	0.72 (3)	Y	6
1423-0310703	WD 1619+525	16 20 24.39	+52 23 21.5	2.596/0.466 (3)	Y	4
1545-0210208	WD 1833+644	18 33 29.22	+64 31 52.2	0.079/1.82 (3)	Y	2
1386-0457478	WD 2224+483	22 26 16.63	+48 37 31.1	∼2 (2)		3
0765-0711730	WD 2318-137	23 21 14.41	-13 27 38.4	∼3 (1)		3
0738-0840954	WD 2341-164	23 44 20.20	-16 10 50.1	6.2-6.7/WDS (2)		7
1165-0040920	WD 0325+263	03 28 03.68	+26 31 52.4	6-6.3/WDS (2)		6
0667-0042912	WD 0357-233	03 59 04.89	-23 12 25.3	1.19 (3)		6
0580-0061995	WD 0358-321	04 00 03.19	-31 57 53.0	∼10 (2)		1
1726-0023464	WD 0725+827	07 36 32.91	+82 36 46.9	∼5 (2)	Y	0
1187-0163669	WD 0824+288	08 27 05.14	+28 44 02.7	0.08/3.33 (3)	Y	7
1394-0199142	WD 0842+496	08 46 23.43	+49 25 36.7	5 (2)	Y	4

Table A3. Candidate list. Entries are arranged by increasing order of the USNO-B1.0 prefix and, within each prefix, by increasing RA. The prefix indicates the distance from the southern pole in increments of 0.1°. The last column provides a subjective assessment of the USNO-B1.0 images, either compact (c) or extended (e). Ambiguous instances have been left blank. Multiple objects on the images are noted where there is a possibility of confused readings. The last column further indicates availability of SDSS data.

USNO-B1.0	eqnx. J2000, epoch J2000 ($^h\ ^m\ ^s.\ \pm\ ^\circ\ '\ ''.$)	No. obs.	PA (°) **R1-B1**	PA (°) **R2-B2**	PA (°) **I2-B2**	Vec. mag. **R1-B1** (arcsec)	Vec. mag. **R2-B2** (arcsec)	Vec. mag. **I2-B2** (arcsec)	USNO-B1.0 images, SDSS data
0034-0006865	03 34 23.39 -86 31 53.87	4		284.0	266.4		0.45	0.64	c
0034-0006916	03 36 18.42 -86 32 05.82	4		11.3	36.4		0.46	0.47	c
0035-0006480	03 26 04.95 -86 26 02.40	4		312.0	305.4		0.69	0.76	c
0035-0006483	03 26 24.16 -86 24 35.65	4		223.3	209.2		0.47	0.57	c
0035-0006625	03 30 36.61 -86 29 28.38	4		185.5	189.6		0.83	1.02	c
0035-0006702	03 32 54.71 -86 29 44.03	4		206.1	226.1		0.52	0.72	c
0035-0007013	03 44 10.02 -86 24 51.29	4		136.6	110.2		0.51	0.84	c
0036-0007224	03 23 50.75 -86 20 56.59	4		71.9	65.4		0.48	1.06	
0036-0007247	03 24 33.90 -86 22 34.49	4		240.9	228.0		0.51	1.36	
0036-0007724	03 39 21.95 -86 20 38.25	4		231.5	238.8		0.50	0.50	c
0036-0008100	03 51 14.50 -86 18 37.49	4		89.0	72.3		0.56	1.05	e
0037-0007134	03 20 47.13 -86 15 51.75	4		176.3	167.7		0.46	0.56	c
0037-0007263	03 25 07.19 -86 14 03.36	4		195.5	193.4		0.49	0.69	c
0037-0007345	03 27 42.47 -86 14 58.75	4		267.6	277.9		0.47	0.80	c
0038-0007574	03 37 31.44 -86 07 36.70	4		323.0	327.7		0.66	0.67	c
0039-0006764	03 22 07.96 -86 03 28.69	4		248.4	278.0		0.46	0.58	e
0039-0006822	03 24 21.95 -86 02 16.30	4		43.0	45.5		1.03	1.68	
0039-0007090	03 33 13.88 -86 02 13.49	4		236.9	231.7		0.59	0.85	e
0039-0007209	03 37 18.24 -86 01 33.75	4		225.0	220.4		0.45	0.80	c
0039-0007813	03 55 27.13 -86 02 53.23	4		216.5	230.2		0.67	0.78	c
0040-0007055	03 23 08.83 -85 56 06.63	4		31.7	21.4		0.80	0.99	
0040-0007079	03 23 48.42 -85 55 50.45	4		43.9	50.9		1.12	1.24	
0040-0007440	03 34 40.62 -85 54 25.42	4		222.3	199.6		0.59	0.96	e
0040-0007463	03 35 41.76 -85 59 36.79	4		46.3	38.0		0.61	1.22	e
0040-0007494	03 36 23.31 -85 56 55.05	4		35.2	42.0		0.54	0.82	e
0040-0007607	03 39 48.88 -85 55 19.06	4		321.7	332.3		0.55	0.69	e
0040-0007650	03 41 12.66 -85 59 47.48	4		174.9	191.9		0.56	0.58	e
0040-0008096	03 53 03.94 -85 57 58.69	4		81.0	65.2		0.58	1.00	e
0041-0007489	03 27 51.71 -85 49 50.45	4		189.3	173.1		0.56	0.58	c
0041-0007524	03 29 05.75 -85 52 51.31	4		207.1	194.5		0.48	0.84	c
0041-0007540	03 29 56.67 -85 50 38.37	4		203.3	197.1		0.78	0.82	e
0041-0007589	03 31 17.98 -85 53 32.22	4		70.8	95.9		0.46	0.58	
0041-0007670	03 34 18.60 -85 52 26.38	4		248.2	249.0		0.54	0.56	e
0041-0007801	03 38 16.01 -85 48 58.35	4		35.0	51.5		0.49	0.63	c
0041-0007853	03 40 04.92 -85 50 34.61	4		185.0	207.1		0.57	0.92	c
0041-0007916	03 41 30.37 -85 49 22.88	4		241.2	273.1		0.46	0.56	e.
0041-0007992	03 43 34.17 -85 49 36.71	4		297.7	271.1		0.45	0.50	c
0042-0007934	03 30 52.83 -85 47 48.94	4		122.7	121.6		0.50	0.67	c
0042-0008005	03 33 40.39 -85 46 42.21	4		353.7	0.0		0.82	0.92	e
0042-0008079	03 35 51.82 -85 47 16.22	4		69.7	60.0		0.90	1.04	c
0042-0008136	03 37 30.59 -85 46 18.71	4		64.4	84.9		0.51	0.56	e
0042-0008199	03 39 44.20 -85 45 59.74	4		163.4	186.8		0.59	0.67	e
0500-0838052	22 38 28.84 -39 54 45.28	4		139.6	148.2		0.62	1.80	e
0501-0828963	22 39 24.19 -39 50 11.80	4		199.9	198.2		0.62	0.67	c
0502-0839757	22 39 24.45 -39 43 00.74	4		288.2	310.0		0.64	0.89	e
0503-0821145	22 39 30.94 -39 39 54.60	4		54.9	34.3		0.66	1.03	c
0503-0821243	22 40 8.81 - 39 40 50.99	4		277.7	290.6		0.52	0.82	c
0504-0831027	22 38 21.38 -39 35 35.90	4		306.0	319.8		0.68	1.43	e
0504-0831304	22 40 08.99 -39 31 57.99	4		233.9	240.4		0.46	0.59	c
0505-0818836	22 38 15.94 -39 26 49.66	4		309.6	330.5		0.45	0.53	c
0505-0818918	22 38 37.35 -39 29 18.48	4		357.9	13.0		0.54	0.80	c
0505-0819180	22 40 15.88 -39 27 42.32	4		294.9	264.6		0.45	0.53	e
0507-0816170	22 39 18.00 -39 14 04.60	4		12.3	353.5		0.47	0.53	c
0507-0816211	22 39 33.85 -39 15 00.52	4		6.8	4.3		0.59	0.66	c
0507-0816304	22 39 59.28 -39 16 17.55	4		70.4	67.1		0.48	0.56	c
0507-0816437	22 40 48.17 -39 13 37.22	4		276.2	294.0		0.46	0.49	c
0527-0283790	10 06 49.87 -37 17 24.46	4		142.8	136.8		0.68	0.69	e
0528-0283777	10 06 02.02 -37 07 40.82	4		93.4	100.7		0.67	0.75	e

Table A3 – *continued* Candidate list.

USNO-B1.0	eqnx. J2000, epoch J2000 ($^h\ ^m\ ^s.\ \pm\ ^\circ\ '\ ''.$)	No. obs.	PA (°) **R1-B1**	PA (°) **R2-B2**	PA (°) **I2-B2**	Vec. mag. **R1-B1** (arcsec)	Vec. mag. **R2-B2** (arcsec)	Vec. mag. **I2-B2** (arcsec)	USNO-B1.0 images, SDSS data
0528-0283958	10 06 28.75 -37 11 57.48	4		316.6	309.5		2.04	2.86	e
0528-0284188	10 06 58.73 -37 09 47.04	4		187.3	166.4		0.47	0.60	c
0528-0284338	10 07 14.49 -37 11 15.04	4		343.1	320.3		0.48	0.61	e
0529-0277001	10 05 54.80 -37 02 48.15	4		217.1	225.8		0.83	1.03	e
0529-0277033	10 05 58.06 -37 05 53.39	4		270.5	260.0		1.17	1.78	e
0529-0277044	10 05 59.77 -37 03 16.30	4		107.3	97.5		0.47	0.53	e
0529-0277813	10 07 42.22 -37 04 55.50	4		214.6	219.4		0.51	0.65	e
0530-0039917	03 07 46.17 -36 59 29.24	4		29.1	26.9		0.70	0.73	c
0531-0039963	03 06 59.88 -36 51 06.92	4		58.4	67.9		0.76	1.78	e
0534-0033956	03 04 57.23 -36 33 15.53	4		135.9	167.1		0.47	0.49	c
0535-0026245	03 05 19.05 -36 27 43.74	4		257.7	261.5		0.47	0.48	c
0536-0025111	03 06 36.93 -36 22 00.77	4		358.8	355.1		0.47	0.47	e
0571-0375276	12 40 00.91 -32 48 03.75	4		51.0	48.5		0.48	0.81	e
0572-0382482	12 40 26.13 -32 43 59.17	4		112.1	112.9		0.69	1.77	e
0574-0375910	12 39 51.13 -32 31 56.00	4		314.3	312.7		1.16	1.22	e
0574-0376072	12 40 20.12 -32 35 23.90	5	344.5	330.9	347.6	0.98	0.41	0.42	c
0630-0013411	00 52 16.45 -26 56 02.09	4		117.5	112.8		0.54	0.54	c
0814-0341014	17 24 40.51 -08 34 28.42	5	293.4	314.1	300.6	0.48	0.45	1.53	e
0814-0341131	17 24 49.97 -08 30 06.85	4	273.0		272.1	0.58		0.82	c
0815-0344448	17 24 16.84 -08 24 39.76	5	284.6	287.8	288.9	1.23	1.61	2.01	c
0816-0364222	17 24 06.14 -08 21 31.70	5	250.2	254.1	276.6	0.80	0.44	1.30	c
0816-0364339	17 24 15.05 -08 19 11.23	5	170.1	178.6	166.6	0.41	0.41	0.43	c
0816-0364528	17 24 27.29 -08 21 42.19	5	168.0	175.9	185.2	0.82	0.83	1.09	c
0816-0364695	17 24 39.93 -08 23 29.39	5	266.8	263.5	274.8	0.53	0.44	0.59	c
0816-0364783	17 24 47.64 -08 21 34.04	5	59.2	55.0	34.6	0.49	0.49	0.55	c
0816-0364857	17 24 53.97 -08 21 38.94	5	256.0	264.6	271.7	0.58	1.17	1.04	c
0816-0364905	17 24 58.50 -08 19 08.07	5	284.0	291.6	280.9	0.66	0.52	0.58	c
0816-0364932	17 25 00.99 -08 21 36.13	4	281.2	266.7		0.72	0.69		c
0817-0389673	17 24 43.23 -08 16 01.28	5	196.1	182.4	213.3	0.40	0.47	0.73	c
0924-0009909	00 44 22.53 +02 29 49.38	5	339.4	351.1	332.0	0.74	0.84	1.11	e/ SDSS
0966-0584913	21 27 51.05 +06 39 50.63	4	119.9	108.4		1.08	0.89		e/SDSS
0969-0633655	21 27 36.75 +06 59 24.69	4		205.5	206.3		0.72	1.06	c/SDSS
0969-0633980	21 28 26.31 +06 58 37.56	5	92.1	82.7	86.3	0.54	0.47	0.46	e/ SDSS
0969-0634114	21 28 51.73 +06 57 47.38	5	204.7	195.0	174.9	0.67	0.73	0.90	e/ SDSS
0970-0663419	21 28 14.66 +07 00 50.71	5	88.8	46.1	76.8	0.98	0.36	0.48	c/SDSS
0971-0681235	21 27 26.09 +07 10 06.27	5	207.6	232.7	232.3	0.47	0.48	0.56	c/e / SDSS
0971-0681479	21 28 02.38 +07 10 16.19	4		269.0	264.2		0.58	0.59	c/e/SDSS
0971-0681705	21 28 36.68 +07 08 47.92	4		21.4	18.6		2.28	3.07	mult. objs./ SDSS
0972-0698506	21 28 29.27 +07 16 14.50	5	188.2	214.6	242.9	1.33	0.35	0.44	c/e/SDSS
0984-0266003	14 31 54.05 +08 25 59.85	4		192.5	211.1		0.46	0.68	e/SDSS
1006-0190377	11 03 11.19 +10 39 32.61	5	0.9	358.8	5.7	0.62	0.48	0.40	SDSS
1006-0190380	11 03 13.15 +10 37 53.11	4		340.4	311.0		0.48	0.61	c/SDSS
1009-0036682	04 03 26.36 +10 57 33.52	4	16.4	43.5		0.64	0.55		e
1009-0190583	11 03 05.92 +10 56 57.01	4		150.8	167.4		0.49	0.59	c/SDSS
1009-0190822	11 04 35.74 +10 57 46.08	5	230.1	257.7	276.2	0.56	0.47	0.55	e/SDSS
1010-0189647	11 03 17.04 +11 02 19.09	4		236.5	232.6		0.82	0.91	c/SDSS
1010-0189899	11 04 57.61 +11 01 50.25	5	310.6	276.6	277.0	0.55	0.43	0.41	c/SDSS
1011-0036127	04 02 26.56 +11 09 06.87	5	171.1	180.0	209.0	0.52	0.43	0.64	c
1011-0036201	04 03 06.37 +11 08 42.15	4	249.2	263.2		1.29	1.10		e
1012-0035157	04 01 57.24 +11 15 07.65	4		303.7	297.9		0.47	0.58	c
1012-0035331	04 03 08.19 +11 15 47.12	4		256.0	268.9		0.45	0.52	c
1053-0170335	08 35 36.61 +15 19 47.67	5	142.0	151.9	139.1	1.04	0.49	0.60	e/SDSS
1053-0170642	08 36 47.71 +15 22 10.66	5	280.4	246 .0	255.8	0.50	0.59	0.65	e/SDSS
1054-0169679	08 35 39.14 +15 25 35.39	4		312.2	309.9		0.88	1.68	e/SDSS
1055-0172337	08 37 22.32 +15 30 36.62	5	138.5	153.4	160.0	0.94	0.96	1.07	e/SDSS
1058-0172600	08 36 25.34 +15 51 11.22	5	181.5	186.8	190.9	0.38	0.50	0.53	e/SDSS
1058-0172658	08 36 50.58 +15 48 58.61	5	232.1	251.2	250.3	0.57	0.56	0.45	e/SDSS
1108-0181990	09 33 44.39 +20 53 00.40	4		268.1	274.4		0.92	1.04	e/SDSS
1169-0233621	12 51 33.52 +26 55 08.74	5	237.7	238.8	263.7	0.45	0.50	1.10	e/SDSS
1170-0240143	12 50 34.32 +27 00 59.22	5	265.6	259.3	284.3	0.39	0.38	0.53	c/SDSS
1188-0095610	05 45 12.60 +28 49 57.91	4	255.5		270.7	0.64		0.82	e

Table A3 – *continued* Candidate list.

USNO-B1.0	eqnx. J2000, epoch J2000 ($^h\ ^m\ ^s.\ \pm\ ^\circ\ '\ ''.$)	No. obs.	PA (°) **R1-B1**	PA (°) **R2-B2**	PA (°) **I2-B2**	Vec. mag. **R1-B1** (arcsec)	Vec. mag. **R2-B2** (arcsec)	Vec. mag. **I2-B2** (arcsec)	USNO-B1.0 images, SDSS data
1188-0095741	05 45 26.13 +28 53 05.66	5	183.7	150.5	165.6	0.46	0.53	0.76	e
1188-0096051	05 46 01.32 +28 50 50.21	5	76.5	74.1	52.6	0.73	0.44	0.64	e
1188-0096357	05 46 33.09 +28 53 06.91	5	228.6	208.2	194.9	1.01	0.61	0.62	c
1189-0098019	05 44 45.47 +28 55 59.58	5	25.7	65.3	49.1	0.60	0.67	0.89	c/SDSS
1189-0098459	05 45 34.05 +28 59 58.33	5	243.0	245.6	269.2	1.21	0.48	0.70	e/SDSS
1189-0098521	05 45 40.95 +28 55 29.41	5	195.6	176.2	187.8	0.45	0.45	0.67	c
1189-0098637	05 45 56.05 +28 56 27.47	5	263.4	281.0	289.4	0.52	0.73	1.14	c
1189-0098790	05 46 14.06 +28 54 22.38	5	195.5	229.6	170.5	0.37	0.35	0.49	c
1190-0098093	05 45 21.49 +29 05 33.14	4	78.3		85.6	0.64		1.55	c/SDSS
1190-0098147	05 45 26.81 +29 05 42.97	5	266.8	241.1	258.7	1.24	0.66	1.17	e/SDSS
1190-0098184	05 45 30.60 +29 05 07.27	5	190.0	164.6	169.6	0.52	0.60	1.00	e/SDSS
1191-0099312	05 45 51.34 +29 07 20.39	5	237.9	203.0	217.6	0.51	0.43	0.44	e/SDSS
1251-0258748	17 33 39.50 +35 11 23.06	5	119.4	107.2	124.9	0.55	1.02	1.36	e/SDSS
1251-0259277	17 35 16.84 +35 09 32.76	5	324.9	277.4	-90.0	0.45	0.54	0.46	c
1252-0258837	17 34 35.38 +35 17 25.89	5	308.1	264.3	274.6	0.47	0.40	0.50	c/SDSS
1253-0259828	17 34 20.46 +35 19 41.06	5	244.7	256.5	254.2	0.40	0.77	1.10	c/SDSS
1254-0260615	17 34 14.52 +35 27 45.51	5	296.6	274.9	266.8	0.49	0.94	0.89	e/SDSS
1254-0261066	17 35 42.50 +35 26 46.43	5	61.7	74.5	87.7	0.44	0.49	0.49	c/e
1254-0261346	17 36 31.45 +35 25 41.54	5	60.8	93.3	98.7	0.39	0.35	0.39	c
1256-0261542	17 34 58.90 +35 40 57.35	5	310.0	291.3	293.9	0.90	0.44	0.77	e
1269-0556127	22 06 50.33 +36 57 38.01	5	122.6	105.5	121.9	0.59	0.37	0.53	c
1270-0576341	22 06 10.07 +37 00 21.47	4	156.2	157.8		0.47	0.48		e
1270-0576530	22 06 34.86 +37 00 09.77	4	79.4	80.4		1.30	0.72		e
1271-0601107	22 06 32.34 +37 06 09.04	5	31.2	35.3	4.9	0.39	0.59	0.70	c
1271-0601311	22 06 57.54 +37 10 04.65	5	268.9	272.7	277.3	0.51	0.85	1.34	c
1271-0601577	22 07 25.96 +37 08 38.91	5	257.2	235.6	234.7	0.68	0.42	0.50	e
1304-0186904	08 01 13.07 +40 24 24.51	5	282.5	250.8	230.5	0.37	0.46	0.44	c/SDSS